

AD-A236 565



2

Report No. NADC-88118-60



**A NEW APPROXIMATE FRACTURE MECHANICS
ANALYSIS METHODOLOGY FOR COMPOSITES
WITH A CRACK OR HOLE**

Hsi C. Tsai and Annette M. Arocho
Air Vehicle And Crew Systems Technology Department (Code 6043)
NAVAL AIR DEVELOPMENT CENTER
Warminster, PA 18974-5000

30 APRIL 1990

PHASE REPORT
Period Covering October 1986 to September 1988
Task No. R02303001
Work Unit No. 133126
Program Element No. 601153N
Project No. BR-23-03-01

DTIC
ELECTE
MAY 17 1991
S D D

Approved for Public Release; Distribution is Unlimited

Prepared for
NAVAL AIR SYSTEMS COMMAND (AIR-931B)
Washington, DC 20361-0001

DTIC FILE COPY

91 5 16 020

91-00042



NOTICES

REPORT NUMBERING SYSTEM — The numbering of technical project reports issued by the Naval Air Development Center is arranged for specific identification purposes. Each number consists of the Center acronym, the calendar year in which the number was assigned, the sequence number of the report within the specific calendar year, and the official 2-digit correspondence code of the Command Officer or the Functional Department responsible for the report. For example: Report No. NADC-88020-60 indicates the twentieth Center report for the year 1988 and prepared by the Air Vehicle and Crew Systems Technology Department. The numerical codes are as follows:

CODE	OFFICE OR DEPARTMENT
00	Commander, Naval Air Development Center
01	Technical Director, Naval Air Development Center
05	Computer Department
10	AntiSubmarine Warfare Systems Department
20	Tactical Air Systems Department
30	Warfare Systems Analysis Department
40	Communication Navigation Technology Department
50	Mission Avionics Technology Department
60	Air Vehicle & Crew Systems Technology Department
70	Systems & Software Technology Department
80	Engineering Support Group
90	Test & Evaluation Group

PRODUCT ENDORSEMENT — The discussion or instructions concerning commercial products herein do not constitute an endorsement by the Government nor do they convey or imply the license or right to use such products.

Reviewed By: *A. Mann* Date: 1/7/91
Branch Head

Reviewed By: *Alvin A. Huang* Date: 1/14/91
Division Head

Reviewed By: *W. J. Smith* Date: 1/15/91
Director/Deputy Director

REPORT DOCUMENTATION PAGE				Form Approved OMB No 0704-0188	
1a REPORT SECURITY CLASSIFICATION UNCLASSIFIED		1b RESTRICTIVE MARKINGS			
2a SECURITY CLASSIFICATION AUTHORITY		3 DISTRIBUTION / AVAILABILITY OF REPORT Approved for Public Release; Distribution is Unlimited			
2b DECLASSIFICATION / DOWNGRADING SCHEDULE					
4 PERFORMING ORGANIZATION REPORT NUMBER(S) NADC-88118-60		5 MONITORING ORGANIZATION REPORT NUMBER(S)			
6a NAME OF PERFORMING ORGANIZATION Air Vehicle and Crew Systems Technology Department		6b OFFICE SYMBOL (if applicable) 6043	7a. NAME OF MONITORING ORGANIZATION		
6c. ADDRESS (City, State, and ZIP Code) NAVAL AIR DEVELOPMENT CENTER Warminster, PA 18974-5000		7b ADDRESS (City, State, and ZIP Code)			
8a. NAME OF FUNDING / SPONSORING ORGANIZATION NAVAL AIR SYSTEMS COMMAND		8b OFFICE SYMBOL (if applicable)	9 PROCUREMENT INSTRUMENT IDENTIFICATION NUMBER		
8c. ADDRESS (City, State, and ZIP Code) Washington DC 20361-0001		10 SOURCE OF FUNDING NUMBERS			
		PROGRAM ELEMENT NO	PROJECT NO	TASK NO	WORK UNIT ACCESSION NO
11. TITLE (Include Security Classification) A New Approximate Fracture Mechanics Analysis Methodology for Composites with a Crack or Hole					
12 PERSONAL AUTHOR(S) Hsi Chin Tsai and Annette M. Arocho					
13a TYPE OF REPORT Phase		13b TIME COVERED FROM 10/86 TO 9/88	14 DATE OF REPORT (Year, Month, Day) 1990 April 30		15 PAGE COUNT
16 SUPPLEMENTARY NOTATION					
17 COSATI CODES			18 SUBJECT TERMS (Continue on reverse if necessary and identify by block number) Equivalent stress intensity factor, Bi-Material Interface, Inherent flaw, Microscopic Model, Anisotropic Model, Fracture Mechanics, Composites		
FIELD	GROUP	SUB-GROUP			
19 ABSTRACT (Continue on reverse if necessary and identify by block number) A new approximate theory which links the inherent flaw concept and the theory of crack tip stress singularities at a bi-material interface has been developed. Three assumptions were made: (1) the existence of inherent flaw (i.e., damage zone) at the tip of the crack was postulated, (2) a fracture of the filamentary composites initiates at a crack lying in the matrix material at the interface of the matrix/filament. (3) a laminate fails whenever the principal load-carrying laminae fails. This will imply that for a laminate consisting of 0° plies, cracks in the matrix perpendicular to the 0° filaments are the triggering mechanism for the final failure. Based on this theory, a parameter \bar{K}_0 which is similar to the stress intensity factor defined for isotropic materials but with a different dimension was defined. Utilizing existing test data, it was found that \bar{K}_0 can be treated as material constant. Based on this finding a fracture strength prediction methodology was developed. The analytical results are correlated well with the test results. This new approximate theory can apply to both brittle and metal matrix composite laminates with crack or hole.					
20 DISTRIBUTION / AVAILABILITY OF ABSTRACT <input checked="" type="checkbox"/> UNCLASSIFIED/UNLIMITED <input type="checkbox"/> SAME AS RPT <input checked="" type="checkbox"/> DTIC USERS			21 ABSTRACT SECURITY CLASSIFICATION		
22a NAME OF RESPONSIBLE INDIVIDUAL Hsi Chin Tsai		22b TELEPHONE (Include Area Code) 215-441-2871		22c OFFICE SYMBOL 6043	

NADC-88118-60

CONTENTS

	Page
FIGURES	vi
TABLES	viii
SYMBOLS	ix
1.0 INTRODUCTION	1
2.0 THEORY	3
3.0 DETERMINATION OF EQUIVALENT STRESS INTENSITY FACTOR \bar{K} , AND INHERENT FLAW SIZE C_0	7
3.1 EQUIVALENT STRESS INTENSIVITY FACTOR, \bar{K}	7
3.2 INHERENT FLAW SIZE, C_0	12
4.0 APPLICATIONS	17
4.1 BORON/ALUMINUM (B/Al) COMPOSITE	17
4.1.1 Notched Strength Prediction	17
4.1.2 Notch Sensitivity of Boron/Aluminum (B/Al) Composite Laminate	26
4.2 GRAPHITE/EPOXY (Gr/Ep) COMPOSITE	26
4.2.1 Notched Strength Prediction/and Notch Sensitivity	33
4.3 GLASS/EPOXY (G/Ep) COMPOSITE	36
4.4 COMPARISON OF ANALYTICAL RESULTS BETWEEN ANISOTROPIC AND MICROSCOPIC MODELS	38
5.0 CONCLUSIONS AND RECOMMENDATIONS	49
5.1 CONCLUSIONS	49
5.2 RECOMMENDATIONS	49
6.0 REFERENCES	51
APPENDIX A CALCULATION OF THE ORDER OF STRESS SINGULARITY AT A BI-MATERIAL INTERFACE	A-1

NADC-88118-60

CONTENTS (Continued)

	Page
APPENDIX B	
CALCULATION OF \bar{K}_Q AND $\frac{\sigma_N}{\sigma_0}$ FOR VARIOUS COMPOSITE LAMINATES	B-1
B.1	
BORON/ALUMINUM COMPOSITE (m = .347)	B-1
B.1.1	
<u>Determination of \bar{K}_Q</u>	B-1
B.1.2	
Determination of \bar{K}_Q From Test Data of Reference 5	B-1
B.1.3	
Prediction of $\frac{\sigma_N}{\sigma_0}$ for Boron/aluminum Laminates with Center Hole	B-3
B.2	
GRAPHITE/EPOXY COMPOSITE (m = .297)	B-4
B.3	
GLASS/EPOXY COMPOSITES (m = .289)	B-4
APPENDIX C	
ANALYTICAL RESULTS OF ANISOTROPIC MODEL	C-1

THIS PAGE INTENTIONALLY LEFT BLANK



Accession For	
NTIS GRA&I	<input checked="" type="checkbox"/>
DTIC TAB	<input type="checkbox"/>
Unannounced	<input type="checkbox"/>
Justification	
By	
Distribution/	
Availability Codes	
Dist	Avail and/or Special
A-1	

NADC-88118-60

FIGURES

Figure		Page
1	Model For Equations For Stresses At A Point Near A Crack	3
2	Crack Normal To The Bi-Material Interface With Inherent Flaw, C_0	6
3	Equivalent Stress Intensity Factor For $[0]_{6T}$ B/Al Composite	14
4	Equivalent Stress Intensity Factor For $[0_2/\pm 45]_s$ B/Al Composite	14
5	Equivalent Stress Intensity Factor for $[\pm 45/0_2]_s$ B/Al Composite	15
6	Equivalent Stress Intensity Factor for $[0/\pm 45]_s$ B/Al Composite	15
7	Comparison Of Predicted And Experimental Notched Strength Results for B/Al $[0]_{6T}$ Composites	19
8	Comparison Of Predicted And Experimental Notched Strength Results for B/Al $[0_2/\pm 45]_s$ Composites	20
9	Comparison Of Predicted And Experimental Notched Strength Results for B/Al $[\pm 45/0_2]_s$ Composites	21
10	Comparison Of Predicted And Experimental Notched Strength Results for B/Al $[0/\pm 45]_s$ Composites	22
11	Notched Strength Prediction For B/Al $[0]_{6T}$ Composite With Center Hole	23
12	Notched Strength Prediction For B/Al $[0_2/\pm 45]_s$ Composite With Center Hole	24
13	Notched Strength Prediction for B/Al $[0/\pm 45]_s$ Composite With Center Hole	25
14	Notch Sensitivities For Various B/Al Laminate Orientations ($w=19.1$ mm)	27
15	Notch Sensitivities For Various B/Al Laminate Orientations ($w=50.8$ mm)	28
16	Notch Sensitivities For Various B/Al Laminate Orientations ($w=101.6$ mm)	29
17	\bar{K}_Q For Gr/Ep With Ply Orientation $[0/\pm 45]_{2s}$	30
18	\bar{K}_Q For Gr/Ep With Ply Orientation $[0/\pm 45]_s$	31
19	\bar{K}_Q For Gr/Ep With Ply Orientation $[0/90/\pm 45]_s$	32
20	Notch Strength And Notch Sensitivities For Various Gr/Ep Laminate Orientations	35
21	\bar{K}_Q For Gl/Ep With Ply Orientation $[0/\pm 45/90]_{2s}$	37
22	Fracture Strength Prediction For Gl/Ep $[0/\pm 45/90]_{2s}$	39

NADC-88118-60

FIGURES (Continued)

Figure		Page
23	Comparison of Analytical Results Between Anisotropic And Microscopic Models B/Al [0] _{6T}	41
24	Comparison of Analytical Results Between Anisotropic And Microscopic Models B/Al [0 ₂ /±45] _s	42
25	Comparison Of Analytical Results Between Anisotropic And Microscopic Models B/Al [±45/0 ₂] _s	43
26	Comparison Of Analytical Results Between Anisotropic And Microscopic Models B/Al [0/±45] _s	44
A-1	Crack Normal To The Bi-Material Interface	A-2

NADC-88118-60

TABLES

Table		Page
1	Equivalent Stress Intensity Factor For $[0]_6T$ B/Al Composite	8
2	Equivalent Stress Intensity Factor For $[0_2/\pm 45]_S$ B/Al Composite	9
3	Equivalent Stress Intensity Factor For $[\pm 45/0_2]_S$ B/Al Composite	10
4	Equivalent Stress Intensity Factor For $[0/\pm 45]_S$ B/Al Composite	11
5	Critical Equivalent Stress Intensity Factor Of Unidirectional B/Al Composite	12
6	Inherent Flaw Size, C_o (mm)	13
7	Fracture Parameters For Various Laminate Configurations Of B/Al	18
8	Fracture Parameters For Various Laminate Configurations Of Gr/Ep	34
9	Comparison Of Analytical Results Between Anisotropic And Microscopic Models B/Al $[0]_6T$	45
10	Comparison Of Analytical Results Between Anisotropic And Microscopic Models $[0_2/\pm 45]_S$	46
11	Comparison Of Analytical Results Between Anisotropic And Microscopic Models $[\pm 45/0_2]_S$	47
12	Comparison Of Analytical Results Between Anisotropic And Microscopic Models $[0/\pm 45]_S$	48
B-1	Unidirectional B/Al Composite Laminates With Center Hole	B-1
B-2	Unidirectional B/Al Composite Laminates With Double Edge Notch	B-2
B-3	Unidirectional B/Al Composite Laminates With Center Slit	B-2
B-4	Fracture Strength Prediction For B/Al $[0]_6T$ With Center Hole	B-2
B-5	Fracture Strength Prediction For B/Al $[0_2/\pm 45]_S$ With Center Hole	B-3
B-6	Fracture Strength Prediction For B/Al $[0/\pm 45]_S$	B-3
B-7	Fracture Parameters Of Gr/Ep Laminate $[0/\pm 45]_{2S}$ With Center Crack	B-4
B-8	Fracture Parameters Of Gr/Ep Laminate $[0/\pm 45]_S$ With Center Crack	B-5
B-9	Fracture Parameters Of Gr/Ep Laminate $[0/90/\pm 45]_S$ With Center Crack	B-5
B-10	Fracture Parameters Of Gl/Ep Laminate $[0/\pm 45/90]_S$ With Center Crack	B-6
B-11	Fracture Strength Prediction Of Gl/Ep Laminate $[0/\pm 45/90]_S$ With Center Hole	B-6

NADC-88118-60

SYMBOLS

σ_N — gross nominal stress

σ_0 — unnotched strength of a composite laminate

R_0 — radius of a hole

a_0 — half crack length

w — width of laminate

r — radius from crack tip

θ — angle measured from x-axis

K — stress intensity factor for isotropic materials

Y — finite width plate correction factor

m — order of singularity

\bar{K} — the equivalent stress intensity factor for composite material

\bar{K}_{AVG} — average value of \bar{K} from a material of all the crack sizes

\bar{K}_Q — critical equivalent stress intensity factor

\bar{K}_{LSF} — \bar{K} derived from C_0 based on least square fit

α — composite parameter

β — composite parameter

ν_1, ν_2 — poisson ratio for medium 1 and 2 respectively

μ_1, μ_2 — shear modulus for medium 1 and 2 respectively

C_0 — inherent flaw size

$$\xi = \frac{2a_0}{w}$$

C_0^* — Inherent flaw size corresponding to an anisotropic model

NADC-88118-60

THIS PAGE INTENTIONALLY LEFT BLANK

NADC-88113-60

1.0 INTRODUCTION

The failure modes associated with fractures in fiber-reinforced composites differ considerably from those of homogeneous isotropic materials. The failure modes in composites are typically in the forms of transverse cracking, delamination, fiber breaks, matrix yielding, matrix cracking, fiber pull-out and fiber/matrix debonding. As a result, it is a very difficult task to predict the fracture process and behavior of composite materials exactly.

In the past, a great deal of effort has been expended to investigate the fracture behavior of composites. A number of fracture mechanics theories have been proposed. These theories have been reviewed and presented extensively in References 1 and 2.

In this report a microscopic theory which was originally proposed by Mar and Lin⁹ has been modified into a new theory. This new theory links the inherent flaw concept³⁻⁸, which postulates that a damage zone exists at the tip of crack, and the theory of crack singularities at a bi-material interface⁹⁻¹². This combined theory can be used to predict the notched strength of organic and metal matrix composites with either a crack or a hole.

The following sections of this report describe the methodology used in the analysis, assumptions taken, analytical results obtained and conclusions made.

NADC-88118-60

2.0 THEORY

The stress distribution at the crack tip in a thin plate for a homogeneous, isotropic elastic solid in terms of the coordinates shown in Figure 1 is given by equation (1)

$$\begin{aligned}\sigma_x &= \sigma_N \left(\frac{a_0}{2r} \right)^{1/2} \left[\cos \frac{\theta}{2} \left(1 - \sin \frac{\theta}{2} \sin \frac{3\theta}{2} \right) \right] \\ \sigma_y &= \sigma_N \left(\frac{a_0}{2r} \right)^{1/2} \left[\cos \frac{\theta}{2} \left(1 + \sin \frac{\theta}{2} \sin \frac{3\theta}{2} \right) \right] \\ \tau_{xy} &= \sigma_N \left(\frac{a_0}{2r} \right)^{1/2} \left[\sin \frac{\theta}{2} \cos \frac{\theta}{2} \cos \frac{3\theta}{2} \right]\end{aligned}\quad (1)$$

where

σ_N = gross nominal stress.

For an orientation directly ahead of the crack ($\theta = 0$)

$$\sigma_x = \sigma_y = \sigma_N \left(\frac{a_0}{2r} \right)^{1/2} \quad \text{and} \quad \tau_{xy} = 0 \quad (2)$$

Irwin¹³ pointed out that equation (1) indicates that the local stresses near a crack depend on the product of the nominal stress and the square root of the half-flaw length. He called this relationship the stress intensity factor K, where for a sharp elastic crack in an infinitely wide plate, K is defined as

$$K = \sigma_N \sqrt{a_0} \quad (3)$$

In the approach using linear-elastic fracture mechanics (LEFM), K is a material parameter and may be determined from tests.

For a finite-width plate, equation (3) is modified to

$$K = Y \sigma_N \sqrt{a_0} \quad (4)$$

Where Y is a parameter that depends on the plate and crack geometry.

To develop a similar concept for composite materials, the assumptions of references 3, 9 were adopted in this paper; i.e.:

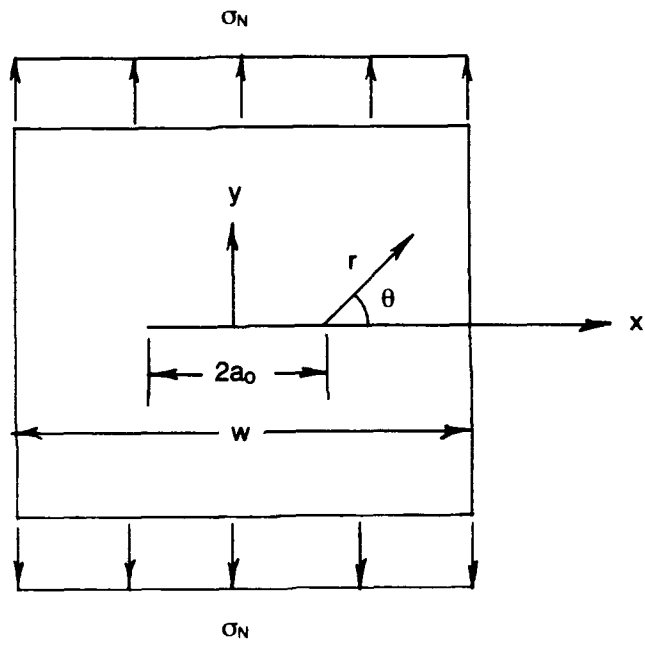


Figure 1. Model For Equations For Stresses At A Point Near A Crack.

NADC-88118-60

- The existence of an inherent flaw (also called a damage zone) at the edge of a hole or at the tip of a crack.
- Fracture of a filamentary composite initiates at a crack lying in the matrix material at the interface of the matrix/filament.
- A laminate fails whenever the principal load-carrying laminae fails. This implies that cracks in the matrix perpendicular to the 0° filaments are the triggering mechanism for the final failure.

Based on the above assumptions, the following theories are developed:

Using the same concept of stress intensity factor as is formulated above for isotropic materials, a material parameter similar to K is defined for composite material as:

$$\bar{K} = Y\sigma_N (a_0)^m \quad (5)$$

where m is the order of singularity of a crack whose tip is at the interface of two different materials as shown in Figure 2. Calculations for determining m are presented in Reference 18.

Note that \bar{K} has a different dimension from K . (K has a dimension of "stress times length to the 1/2 power", while \bar{K} has a dimension of "stress times length to the m power".)

Although some composite materials (such as polymeric matrix composites) fail in a brittle manner, a damage zone does develop which is analogous to the plastic zone for ductile materials. Using this concept in conjunction with equation (5) yields:

$$\bar{K} = Y\sigma_N (a_0 + C_0)^m \quad (6)$$

where C_0 is defined as an inherent flaw size. The term inherent flaw size is used since unnotched strength, σ_0 , of a composite laminate is given by equation (6) for the case of vanishing a_0 .

$$\bar{K} = \sigma_0 (C_0)^m \quad (7)$$

where Y_0 is the correction factor for infinite plate.

It should be noted that C_0 does not physically refer to an inherent crack, but a characteristic dimension of damage zone at the tip of a notch or crack prior to ultimate failure.

The question we may ask now is whether \bar{K} and C_0 are material constants. Before we reach a conclusion, certain equations are helpful in answering this question.

NADC-88118-60

Substituting equation (7) into equation (6), and after some manipulations, we obtain the following important equations that will be used to determine parameter \bar{K} , C_o and notched strength of composite laminates

$$C_o = \frac{a_o}{\left(\frac{\sigma_o}{\bar{Y}\sigma_N}\right)^{1/m} - 1} \quad (8)$$

$$\bar{K} = a_o^m Y_o \sigma_o \left\{ \left(\frac{\bar{Y}\sigma_N}{\sigma_o}\right)^{-1/m} - 1 \right\}^{-m} \quad (9)$$

$$\frac{\sigma_N}{\sigma_o} = \frac{1}{\bar{Y}} \left\{ \frac{C_o}{a_o + C_o} \right\}^m \quad (10)$$

or

$$\frac{\sigma_N}{\sigma_o} = \frac{1}{\bar{Y}} \frac{1}{\left\{ 1 + \left(\frac{Y_o \sigma_o}{\bar{K}}\right)^{1/m} a_o \right\}^m} \quad (11)$$

where

$$\bar{Y} = \frac{Y}{Y_o}$$

In the following sections, \bar{K} will be called the equivalent stress intensity factor for composite materials.

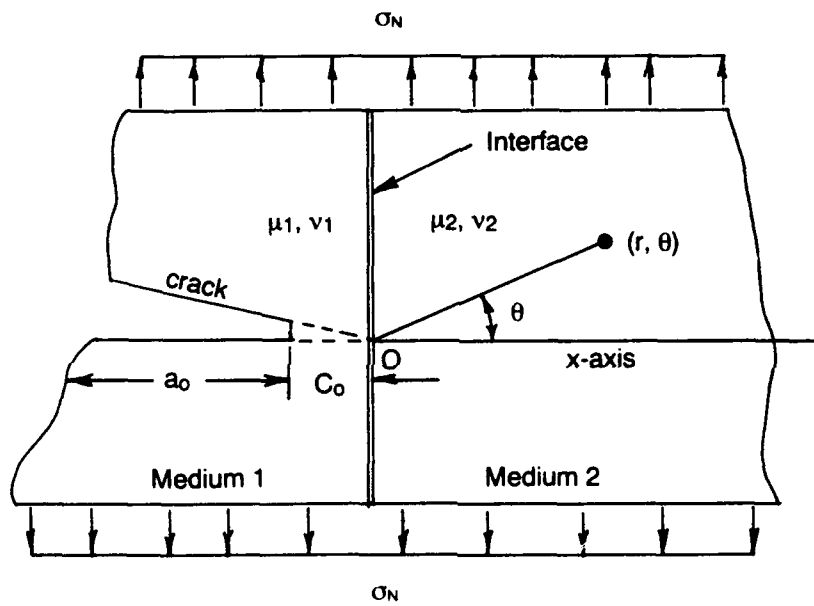


Figure 2. Crack Normal To The Bi-Material Interface With Inherent Flaw, C_o .

NADC-88118-60

3.0 DETERMINATION OF EQUIVALENT STRESS INTENSITY FACTOR, \bar{K} AND INHERENT FLAW SIZE

Reference 8 provides extensive fracture test data of boron/aluminum laminates with various proportions of 0° and $\pm 45^\circ$ plies. Hence, this test data will be used to characterize the fracture behavior of boron/aluminum composite laminates.

3.1 EQUIVALENT STRESS INTENSITY FACTOR, \bar{K}

From Appendix A, the order of stress singularity at the boron/aluminum interface, m equals .347. From equation (9), the equivalent stress intensity factor for boron/aluminum composite laminate with center crack can be written as follows:

$$\bar{K} = a_0^{.347} \sigma_0 \left\{ \left(\frac{Y_{ON}}{\sigma_0} \right)^{-2.88} - 1 \right\}^{-.347} \quad (12)$$

Equation (12) is used to characterize the critical equivalent stress intensity factor of boron/aluminum laminates with various layups.

By using the fracture test results from reference 8, equivalent stress intensity factors were calculated from equation (12) and are tabulated on Tables 1 through 4 for boron/aluminum composite with laminate constructions $[0]_{6T}$, $[0_2/\pm 45]_s$, $[\pm 45/02]_s$ and $[0/\pm 45]_s$ respectively. Note the test results shown in Tables 1 to 4 are average test results of reference 8. As shown in Tables 1 to 4, \bar{K} values seem to be a material property and vary with different laminate orientations. \bar{K} values are also plotted on Figures 3 to 6. \bar{K}_{AVG} is the average value of \bar{K} from all the crack sizes. As shown in the figures, \bar{K}_{AVG} can be approximately treated as a material constant. It has to be pointed out here that \bar{K}_{AVG} was obtained by averaging three different widths of plate. For $w = 101.6\text{mm}$ \bar{K} values are almost the same for different $2a_0/w$ ratios.

The detailed calculations of \bar{K} are shown in Appendix B.1.

NADC-88118-60

Table 1. Equivalent Stress Intensity Factor For [0]6T B/Al Composite.

w (mm)	a _o (mm)	ξ	Y	$\left(\frac{\sigma_N}{\sigma_o}\right)_{TEST}$	\bar{K} (MPa(mm) ^{.347})	$\left(\frac{\sigma_N}{\sigma_o}\right)$	Error %
19.1	.25	.025	1.001	.818	1125.0	.878	7.4
19.1	.65	.068	1.003	.6845	1136.0	.760	11.0
50.8	1.25	.05	1.001	.592	1166	.663	12.0
50.8	2.55	.1	1.006	.555	1455	.546	-1.6
50.8	7.6	.3	1.06	.4003	1479	.3705	-7.5
50.8	12.7	.5	1.189	.3098	1518	.279	-10.0
101.6	2.55	.05	1.001	.580	1455	.549	-5.3
101.6	5.1	.1	1.006	.468	1435	.443	-5.3
101.6	15.25	.3	1.06	.3024	1399	.295	-2.6
101.6	25.4	.5	1.189	.232	1430	.221	-4.7

$$\bar{K}^{AVG} = 1360 \text{ MPa (mm)}^{.347}$$

$$\sigma_o = 1672 \text{ MPa}$$

$$Y = \sqrt{\sec\left(\frac{\pi}{2}\xi\right)}$$

$$\xi = \frac{2a_o}{w}$$

NADC-88118-60

Table 2. Equivalent Stress Intensity Factor For $[0_2/\pm 45]_s$ B/Al Composite.

w (mm)	a_0 (mm)	ζ	Y	$\left(\frac{\sigma_N}{\sigma_0}\right)_{TEST}$	\bar{K} (MPa(mm) ^{3/4})	$\left(\frac{\sigma_N}{\sigma_0}\right)$	Error %
19.1	.25	.025	1.001	.878	652.6	.891	1.5
19.1	.65	.068	1.003	.782	681.9	.782	0.
50.8	1.25	.05	1.001	.721	740.	.686	-4.8
50.8	2.55	.1	1.006	.571	683.1	.570	0.
50.8	7.6	.3	1.06	.395	697.8	.389	-1.5
50.8	12.7	.5	1.189	.274	639.0	.293	7.0
101.6	2.55	.05	1.001	.579	695.1	.572	-1.2
101.6	5.1	.1	1.006	.464	680.6	.464	0.
101.6	15.25	.3	1.06	.321	711.5	.310	-3.5
101.6	25.4	.5	1.189	.229	674.6	.232	1.6

$$\bar{K}^{AVG} = 685.6 \text{ MPa (mm)}^{3/4}$$

$$\sigma_0 = 800.1 \text{ MPa}$$

$$Y = \sqrt{\sec\left(\frac{\pi}{2} \zeta\right)}$$

$$\zeta = \frac{2a_0}{w}$$

NADC-88118-60

Table 3. Equivalent Stress Intensity Factor For [$\pm 45/02$]_s B/Al Composite.

w (mm)	a _o (mm)	ξ	Y	$\left(\frac{\sigma_N}{\sigma_0}\right)_{TEST}$	\bar{K} (MPa(mm) ^{.347})	$\left(\frac{\sigma_N}{\sigma_0}\right)$	Error %
19.1	.25	.025	1.001	-	-	-	-
19.1	.65	.068	1.003	-	-	-	-
50.8	1.25	.05	1.001	.619	674.7	.633	2.3
50.8	2.55	.1	1.006	.531	716.6	.517	-2.6
50.8	7.6	.3	1.06	.361	720.8	.349	-3.5
50.8	12.7	.5	1.189	.245	647.7	.262	7.0
101.6	2.55	.05	1.001	.528	707.6	.520	-1.6
101.6	5.1	.1	1.006	.423	703.8	.417	-1.3
101.6	15.25	.3	1.06	.281	706.2	.276	-1.6
101.6	25.4	.5	1.189	.201	673.0	.207	3.1

$$\bar{K}^{AVG} = 693.8 \text{ MPa(mm)}^{.347}$$

$$\sigma_0 = 910.5 \text{ MPa}$$

$$Y = \sqrt{\sec\left(\frac{\pi}{2} \xi\right)}$$

$$\xi = \frac{2a_0}{w}$$

NADC-88118-60

Table 4. Equivalent Stress Intensity Factor For $[0/\pm 45]_s$ B/Al Composite.

w (mm)	a ₀ (mm)	$\frac{a}{w}$	Y	$\left(\frac{\sigma_N}{\sigma_0}\right)_{TEST}$	\bar{K} (MPa(mm) ^{3/4})	$\left(\frac{\sigma_N}{\sigma_0}\right)$	ERROR %
19.1	.25	.025	1.001	-	-	-	-
19.1	.65	.068	1.003	.828	564.6	.865	4.4
50.8	1.25	.05	1.001	.796	645.8	.789	-1.0
50.8	2.55	.1	1.006	.730	710.1	.688	-5.7
50.8	7.5	.3	1.06	.458	597.8	.481	5.2
50.8	12.7	.5	1.189	.329	563.1	.367	11.5
101.6	2.55	.05	1.001	.699	656.5	.692	-1.0
101.6	5.1	.1	1.006	.620	702.0	.569	-8.2
101.6	15.25	.3	1.06	.413	678.0	.388	-6.0
101.6	25.4	.5	1.189	.271	583.9	.293	8.2

$$\bar{K}^{AVG} = 633.5 \text{ MPa(mm)}^{3/4}$$

$$\sigma_0 = 581.4 \text{ MPa}$$

$$Y = \sqrt{\sec\left(\frac{\pi}{2} \frac{a}{w}\right)}$$

$$\frac{a}{w} = \frac{2a}{w}$$

NADC-88118-60

The above tests are for center crack specimens. For other crack types and locations⁵, the calculated equivalent stress intensity factors are shown on Table 5, condensed from Appendix B.1.2. It can be seen that \bar{K} for these unidirectional boron/aluminum composites is constant for different crack conditions. The reason for the slightly different \bar{K} as compared to Table 1 is due to a different value of ultimate tensile strength.

Table 5. Critical Equivalent Stress Intensity Factor Of Unidirectional B/Al⁵ Composite.

SPECIMEN*	$\frac{2a_0}{w}$ or $\frac{2R}{w}$	\bar{K}_{AVG}	MPa (mm) ^{.347}
CH	.25		1246.00
CS	.40		1227.00
DEN	.30		1237.00

*CH - CENTER HOLE SPECIMEN
 CS - CENTER SPLIT SPECIMEN
 DEN - DOUBLE EDGE NOTCH SPECIMEN

3.2 INHERENT FLAW SIZE, C_0

Two methods were used to calculate the inherent flaw sizes for a composite laminate with center crack.

Least Square Fit

Equation (8), in which C_0 is a proportional constant, can be rearranged to yield

$$a_0 = C_0 \left\{ \left(\frac{Y\sigma_N}{\sigma_0} \right)^{-2.88} - 1 \right\} \quad (13)$$

By using the fracture test data as shown in Tables 1 to 4, and the least square fit, C_0 for various laminate constructions are determined as shown in Table 6.

Average Equivalent Stress Intensity Method

From Equation (7) we have

$$\bar{K}_{AVG} = \sigma_0 (C_0)^m \quad (14)$$

where $m = .347$ for boron/aluminum.

The inherent flaw size can be derived from equation (14) as follows:

NADC-88118-60

$$C_o = \left(\frac{\bar{K}_{AVG}}{\sigma_o} \right)^{1/m} \tag{15}$$

In the case of boron/aluminum composite, equation (15) becomes

$$C_o = \left(\frac{\bar{K}_{AVG}}{\sigma_o} \right)^{2.88} \tag{16}$$

The inherent flaw sizes for various laminate orientations were calculated using this method and were also tabulated on Table 6.

Table 6. Inherent Flaw Size, C_o (mm).

	Least Square Fit	\bar{K}_{AVG} Method
[0] _{6T}	.633	.552
[0 ₂ /±45] _s	.593	.641
[±45/0 ₂] _s	.405	.457
[0/±45] _s	.976	1.28

We pointed out earlier that C_o does not physically refer to an inherent crack, but rather to a characteristic dimension of damage zone at a crack tip, prior to fracture failure. Comparing the dimension of C_o with respect to the crack size of B/Al specimens as shown in Table 1 to 4, it is clear that C_o cannot be neglected in the calculations of equivalent stress intensity factor. The significance of C_o will be further discussed in Section 4.0.

Equation (7) is used to calculate critical equivalent stress intensity factor based on the C_o determined from least square fit method. These values are also plotted on Figures 3 to 6 as \bar{K}_{LSF} . It can be seen from the plots that there is not much difference between \bar{K}_{LSF} and \bar{K}_{AVG} except in the plot for the [0/±45]_s laminates, where though there is a greater difference between \bar{K}_{AVG} and \bar{K}_{LSF} , \bar{K}_{AVG} provides a better result. For this reason \bar{K}_{AVG} will be adopted in this report and will be denoted as \bar{K}_Q .

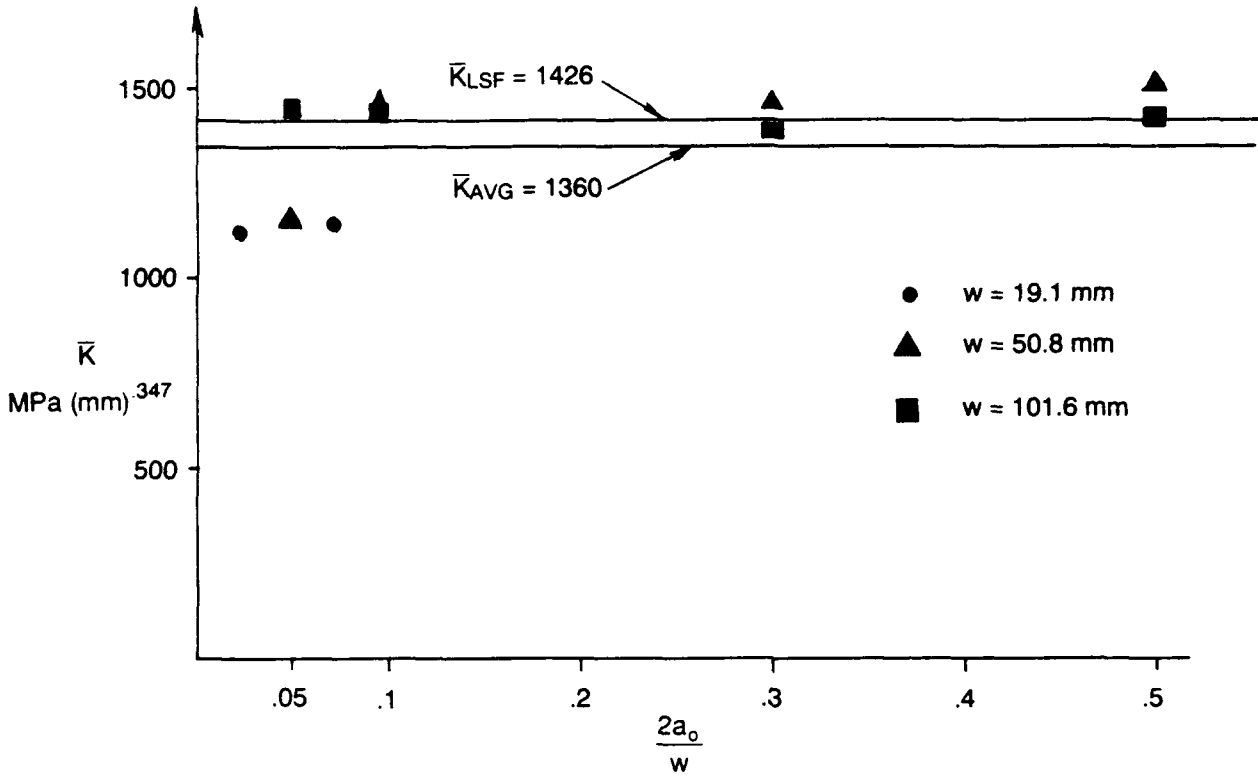


Figure 3. Equivalent Stress Intensity Factor For $[0]_{6T}$ B/Al Composite.

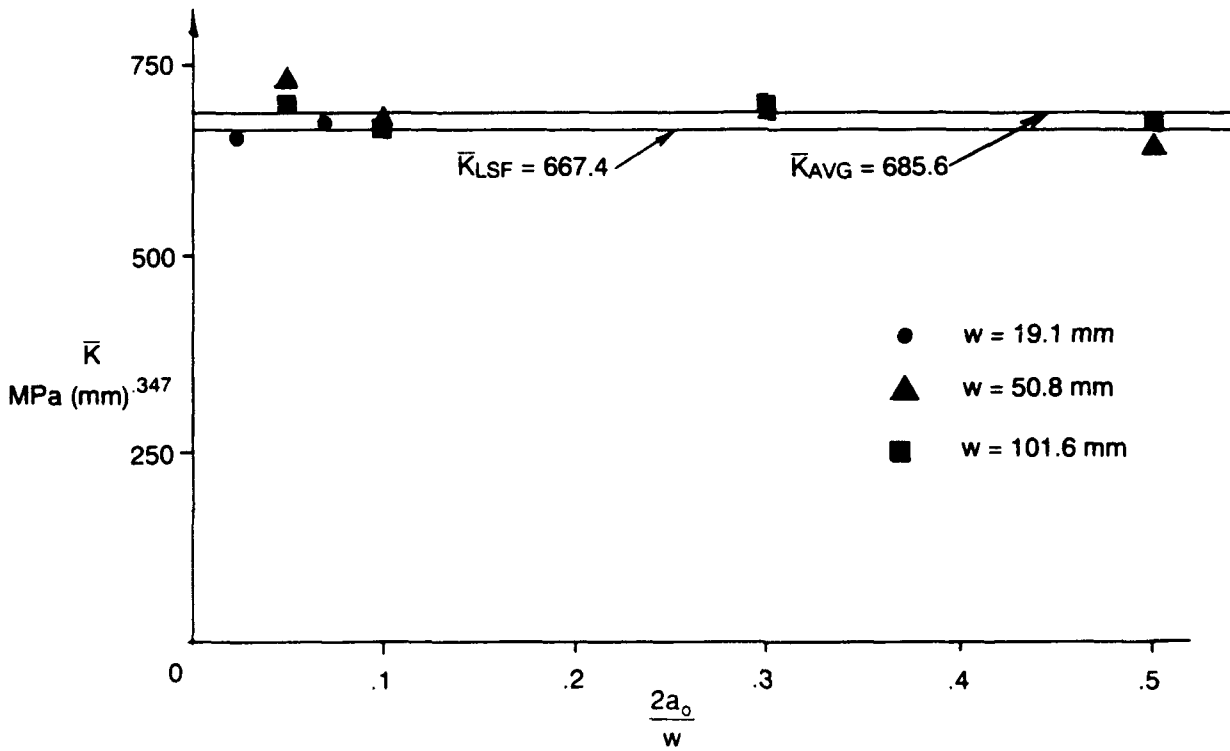


Figure 4. Equivalent Stress Intensity Factor For $[0_2/\pm 45]_s$ B/Al Composite.

NADC-88113-60

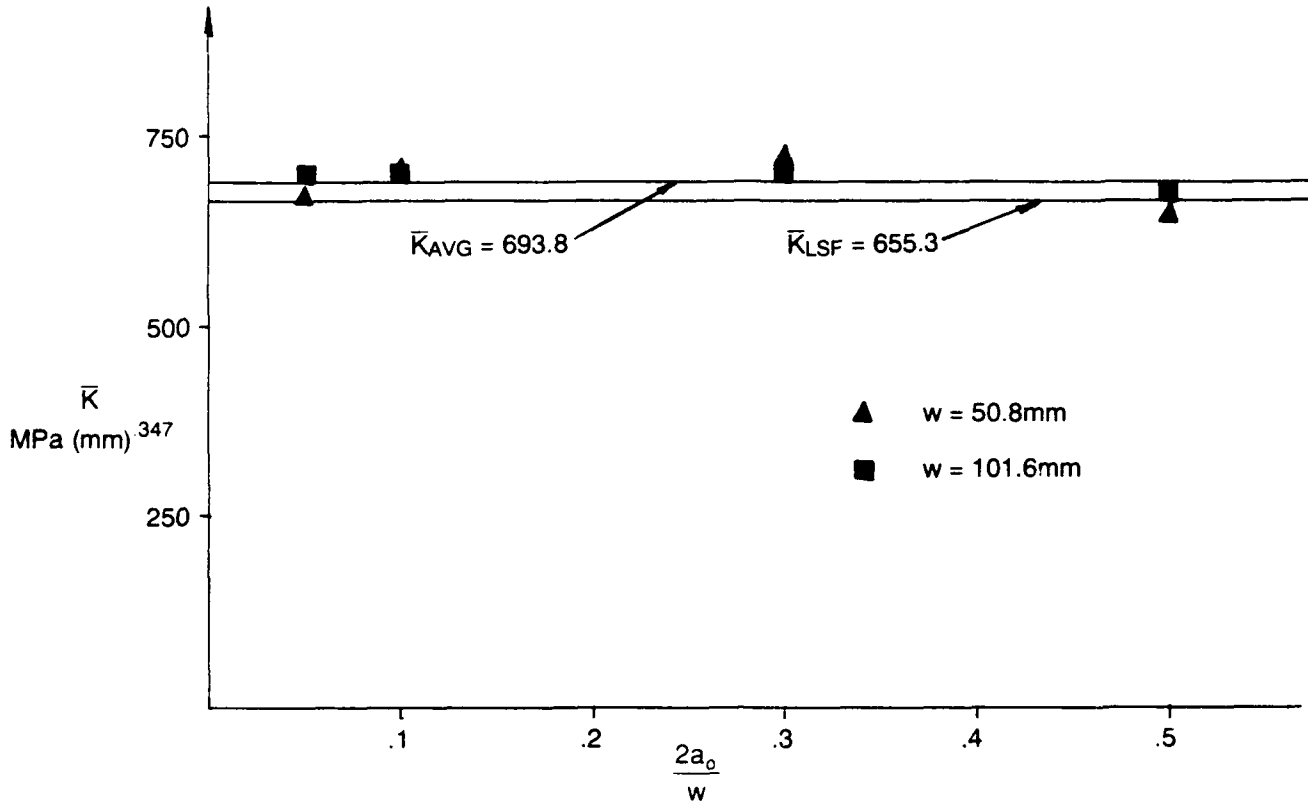


Figure 5. Equivalent Stress Intensity Factor For $[\pm 45/0_2]_s$ B/Al Composite.

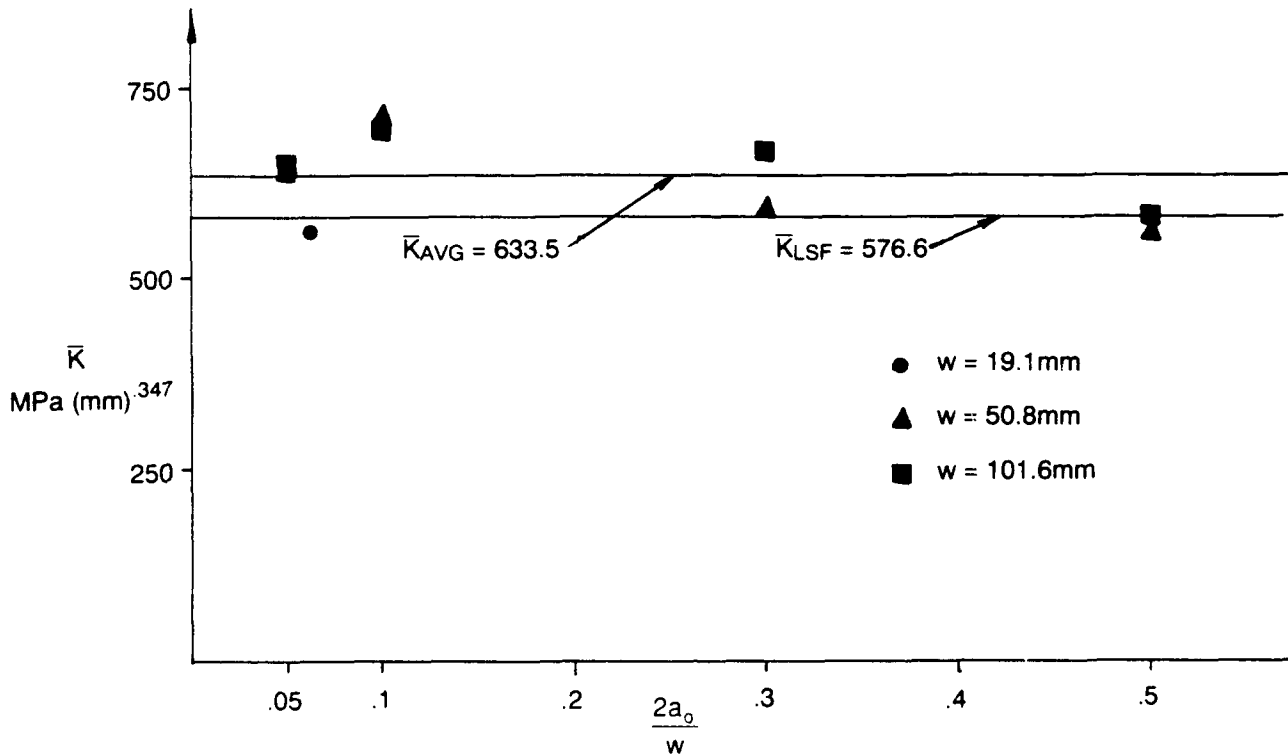


Figure 6. Equivalent Stress Intensity Factor For $[0/\pm 45]_s$ B/Al Composite.

NADC-88118-60

THIS PAGE INTENTIONALLY LEFT BLANK

NADC-88118-60

4.0 APPLICATIONS

Once the critical equivalent stress intensity factor, \bar{K}_Q is known, the fracture strength of the composite laminates can be obtained from equations (10) and (11).

From equation (11), we have a fracture strength prediction formula as follows:

$$\frac{\sigma_N}{\sigma_o} = \frac{1}{Y} \left\{ 1 + \left(\frac{\bar{K}_Q}{Y_o \sigma_o} \right)^{-\frac{1}{m}} a_o \right\}^{-m} \quad (17)$$

From Equation (17), it can be seen that the larger the term $\left(\frac{\bar{K}_Q}{\sigma_o} \right)$, the lesser the notch sensitivity and so from equation (7), we can conclude that the larger the inherent flaw size (i.e., the damage zone size), C_o , the lesser the notch sensitivity.

In the following subsections, the theory developed here will be used to predict the fracture strength of various composite laminates.

4.1 BORON/ALUMINUM (B/Al) COMPOSITE

4.1.1. Notched Strength Prediction

For B/Al composite laminates, $m = .347$ and for a center crack specimen, equation (17) becomes

$$\frac{\sigma_N}{\sigma_o} = \frac{1}{Y} \left\{ 1 + \left(\frac{\bar{K}_Q}{\sigma_o} \right)^{-2.88} a_o \right\}^{-.347} \quad (18)$$

where for a composite laminate with a center crack, Y is assumed to be the same as that for an isotropic material⁸.

$$Y = \left\{ \sec \left(\frac{\pi a_o}{w} \right) \right\}^{1/2}$$

For convenience, data from Tables 1 to 4 and 6 are summarized on Table 7 to be used for the following analysis. Substituting σ_o and \bar{K}_Q from Table 7 for different ply conditions into equation (18) values for $\frac{\sigma_N}{\sigma_o}$ can be obtained for various crack sizes and are tabulated on Column 7 of Tables 1 to 4. The analytical results are also plotted on Figures 7 to 10.

As can be seen, the prediction represents the experimental results reasonably well.

The \bar{K}_Q values obtained from center cracked specimens are also applied to B/Al specimens with center holes. Comparisons of the analytical results and test results¹⁴ are shown in Figures 11 to 13. Figure 11 shows excellent correlation between test and analytical results for $[0]_{6T}$ laminates with center holes, while in Figure 12 and 13, the maximum percentage error for analytical results is around 13%. The detailed calculations are shown in Appendix B.1.3. This confirms the findings of reference 18 and 19 that the length of discontinuity and not the shape appeared to control the fracture strength of composite laminates.

NADC-88118-60

Table 7. Fracture Parameters For Various Laminate Configurations Of B/Al.

Ply Configuration	σ_0 (MPa)	\bar{K}_Q MPa (mm) ^{.347}	$\frac{\bar{K}_Q}{\sigma_0}$ (mm) ^{.347}	C_0 (mm)
[0] _{6T}	1672	1360	.81	.552
[0 ₂ /±45] _s	800.1	685.6	.867	.641
[±45/0 ₂] _s	910.5	693.8	.762	.457
[0/±45] _s	581.4	633.5	1.09	1.28

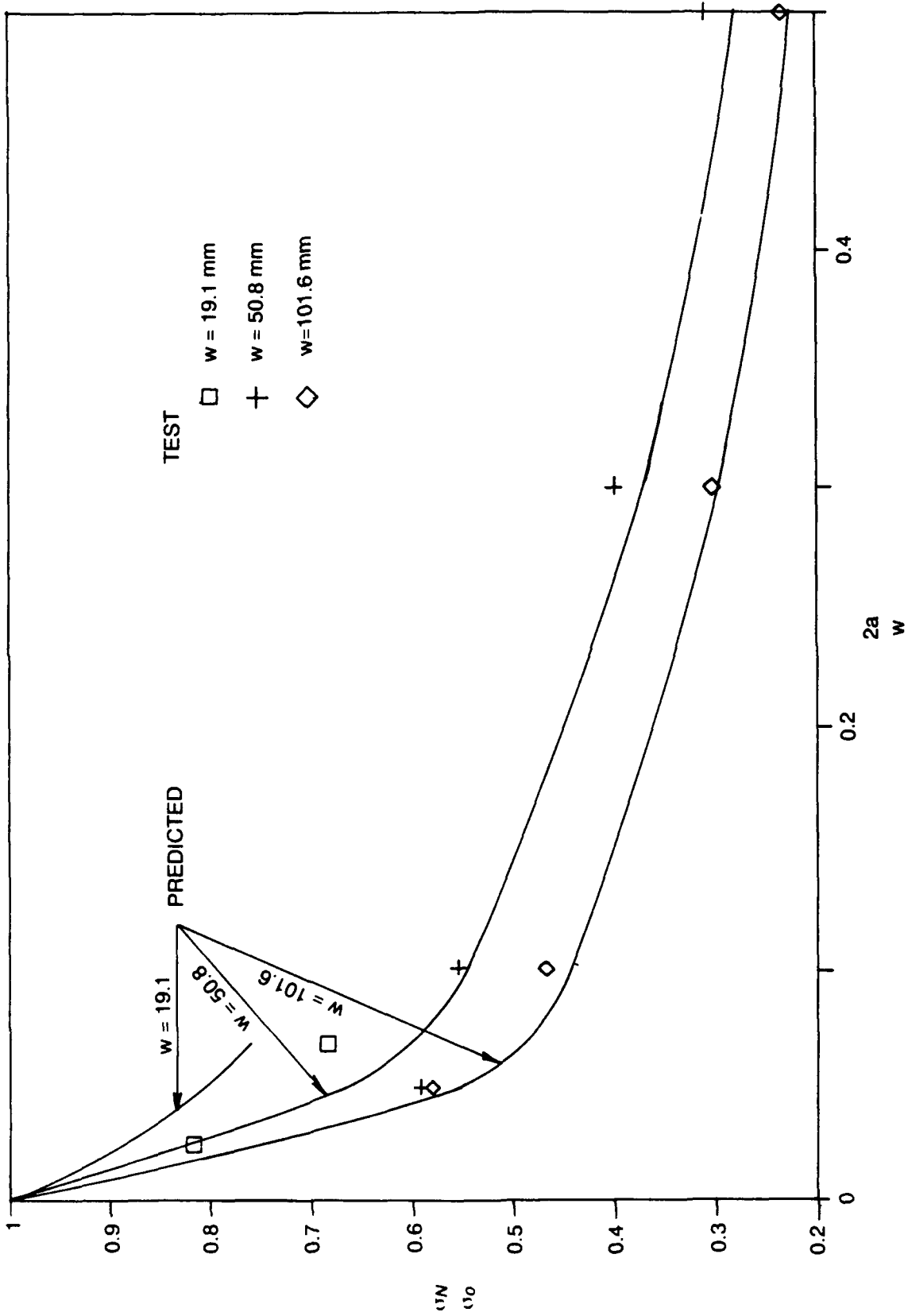


Figure 7. Comparison Of Predicted And Experimental Notched Strength Results For B/Al (0°)6T Composites.

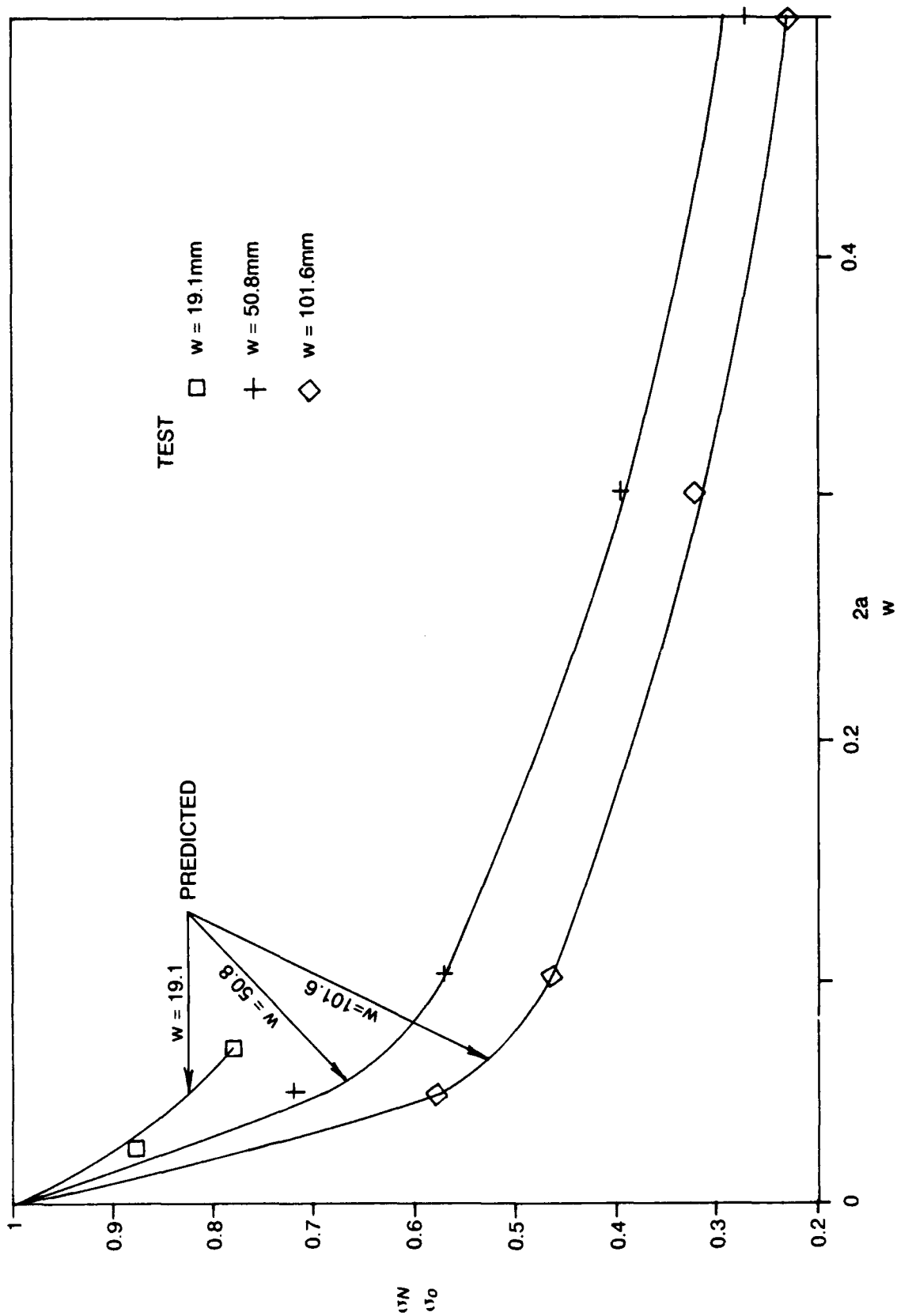


Figure 8. Comparison Of Predicted And Experimental Notched Strength Results For B/AI [02/+45]s Composites.

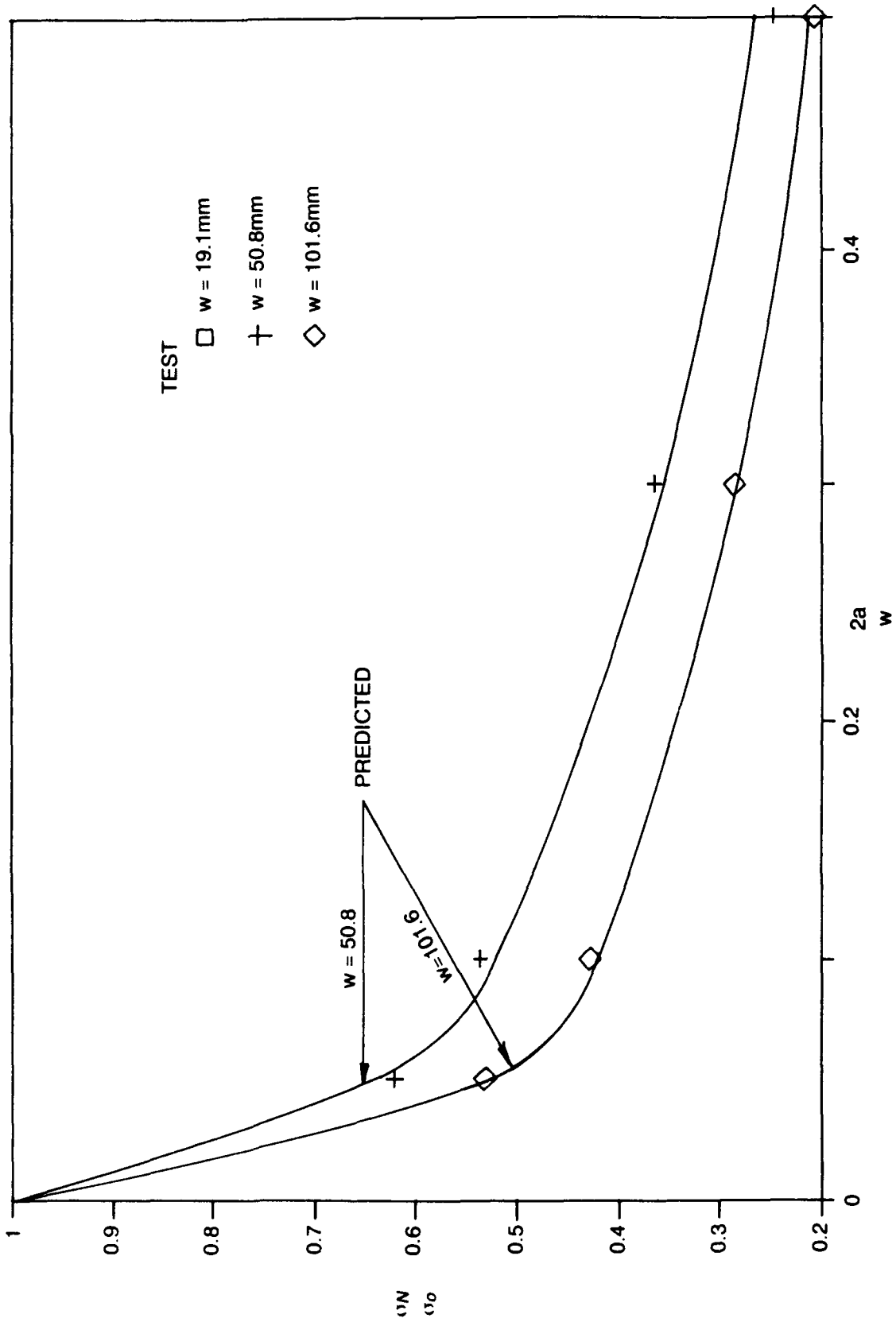


Figure 9. Comparison Of Predicted And Experimental Notched Strength Results For B/AI [-45/0]s Composites.

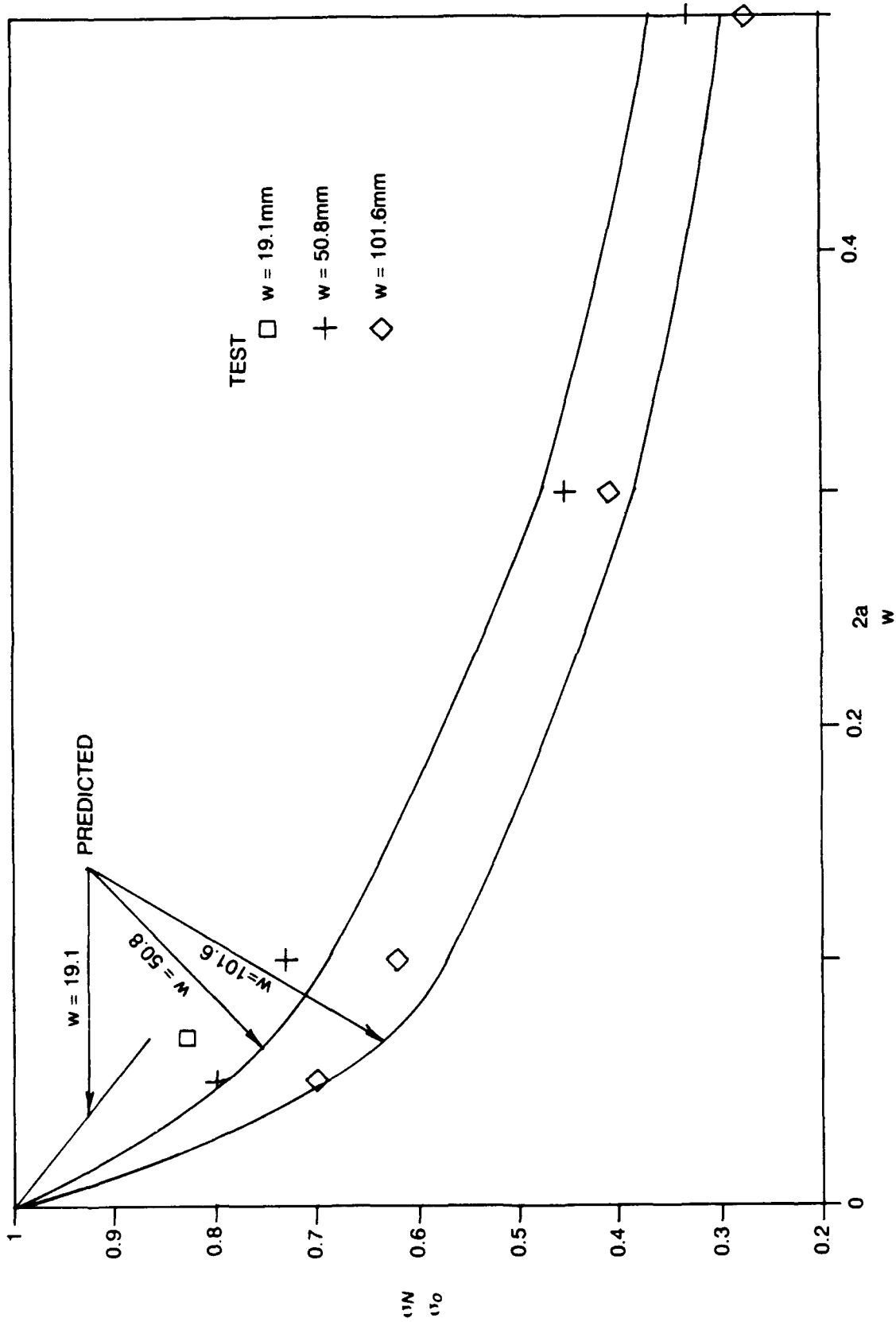


Figure 10. Comparison Of Predicted And Experimental Notched Strength Results For B/AI [0/±45]s Composites.

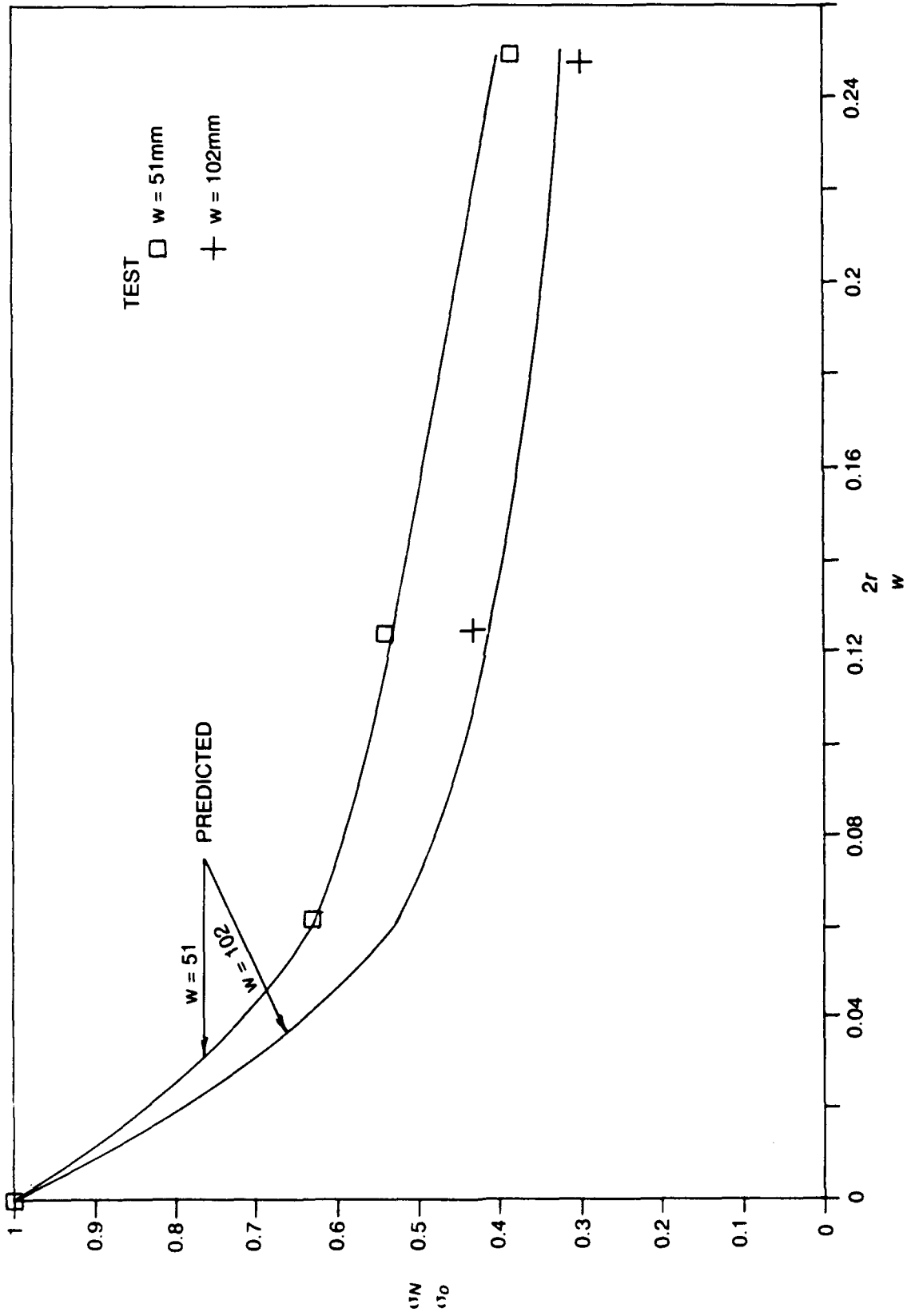


Figure 11. Notched Strength Prediction For B//Al [0]sT Composite With Center Hole.

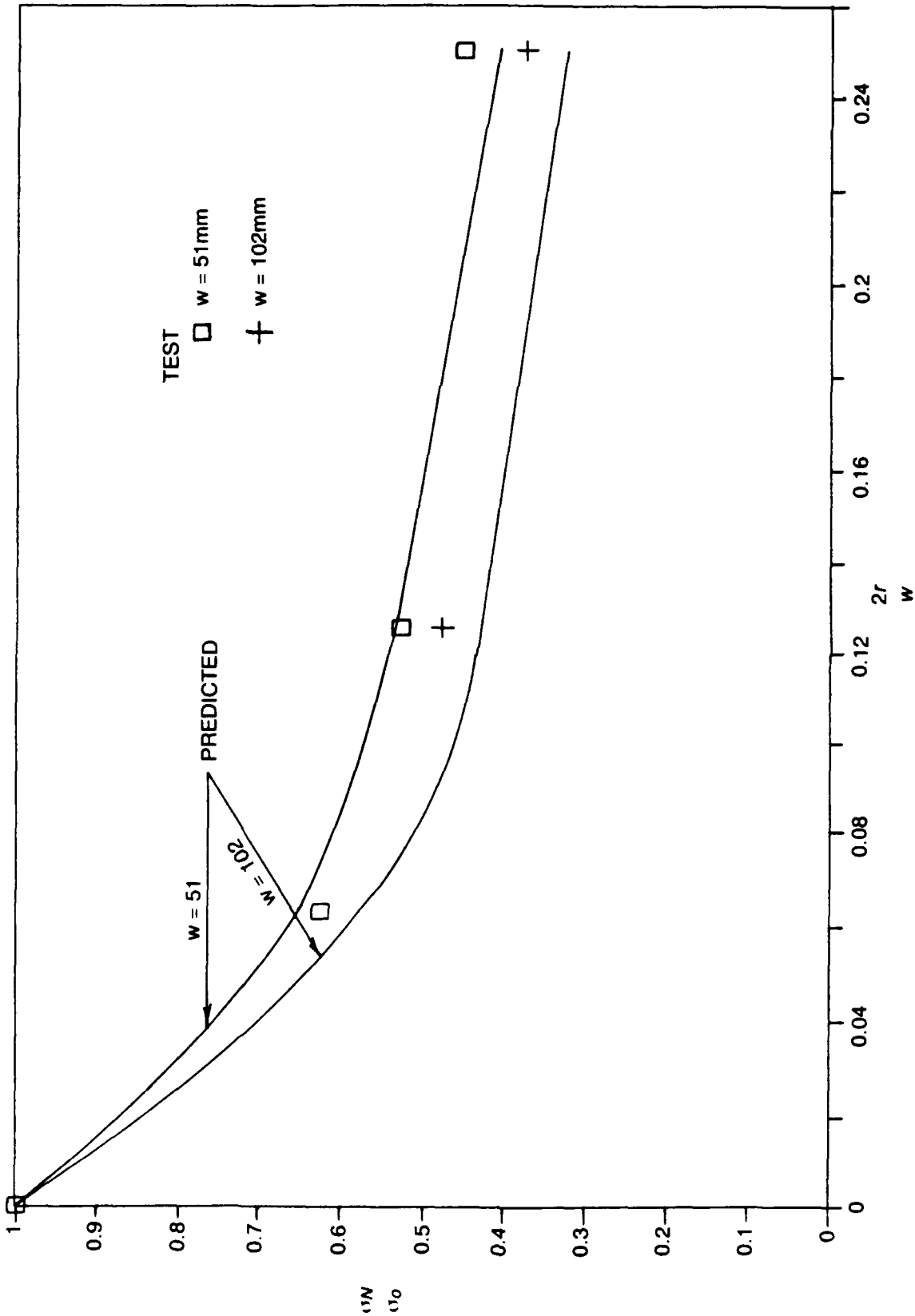


Figure 12. Notched Strength Prediction for B/AI [02/±45]s Composites With Center Hole.

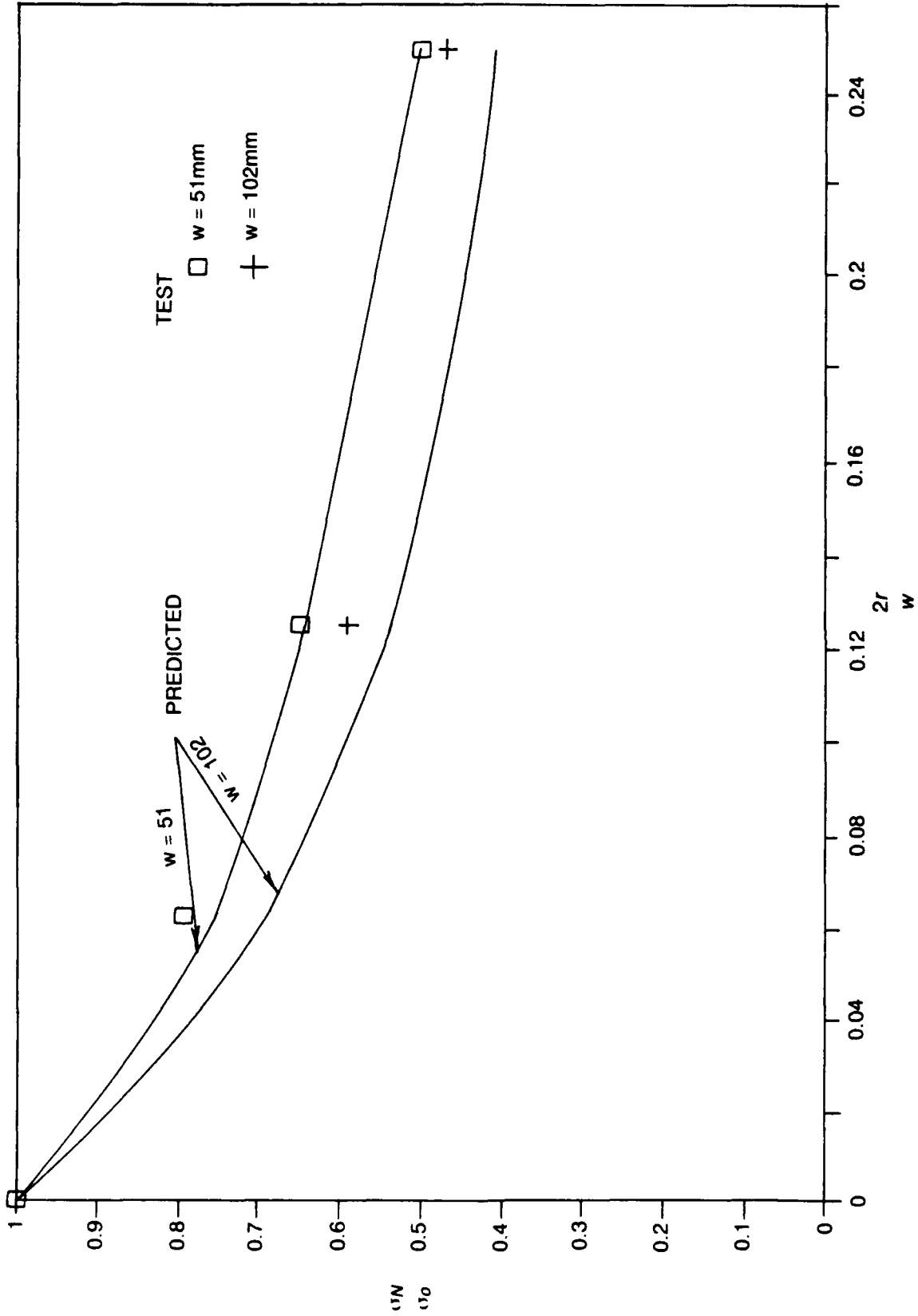


Figure 13. Notched Strength Prediction For B/AI [0/±45]_s Composite With Center Hole.

NADC-88118-60

4.1.2. Notch Sensitivity of Boron/Aluminum (B/Al) Composite Laminate

The $\frac{\sigma_N}{\sigma_0}$ test data in Tables 1 to 4 are plotted on Figures 14 to 16 for composite laminate of various widths to check the notch sensitivity of B/Al composites. It is obvious that $[\pm 45/0_2]_s$ is the most notch-sensitive, while $[0/\pm 45]_s$ is the least sensitive to the notch size. For $\frac{2a_0}{w} \leq .1$, $[0]_{6T}$ is more sensitive to the notch size than $[0_2/\pm 45]_s$. For $\frac{2a_0}{w} > .1$, the $\frac{\sigma_N}{\sigma_0}$ vs $\frac{2a_0}{w}$ curve for $[0]_{6T}$ and $[0_2/\pm 45]_s$ laminates are almost identical. The trend mentioned above can be detected by using a parameter¹⁵ defined by the ratio $\frac{\bar{K}_Q}{\sigma_0}$ as shown in Table 7. The ranking of various laminate configurations for the $\frac{\bar{K}_Q}{\sigma_0}$ index is $[0/\pm 45]_s$, $[0_2/\pm 45]_s$, $[0]_{6T}$ and $[\pm 45/0_2]_s$ in descending order. The relative values of $\frac{\bar{K}_Q}{\sigma_0}$ show a similar trend to that of damage zone size, C_0 .

It can be concluded that the larger the ratio $\frac{\bar{K}_Q}{\sigma_0}$ (or the damage zone size C_0) the less fracture sensitivity there is to the notch size.

4.2 GRAPHITE/EPOXY (Gr/Ep) COMPOSITE

Equation (9) is used to characterize the \bar{K}_Q for Gr/Ep composites.⁶ The detailed calculations are shown in Appendix B.2. \bar{K}_Q for various ply orientations is plotted as shown in Figures 17 to 19. It can be seen that \bar{K}_Q for Gr/Ep composites can be treated as a material constant. Table 8 summarizes the characterization results of Gr/Ep composite laminates. For Gr/Ep, $m = .297$.

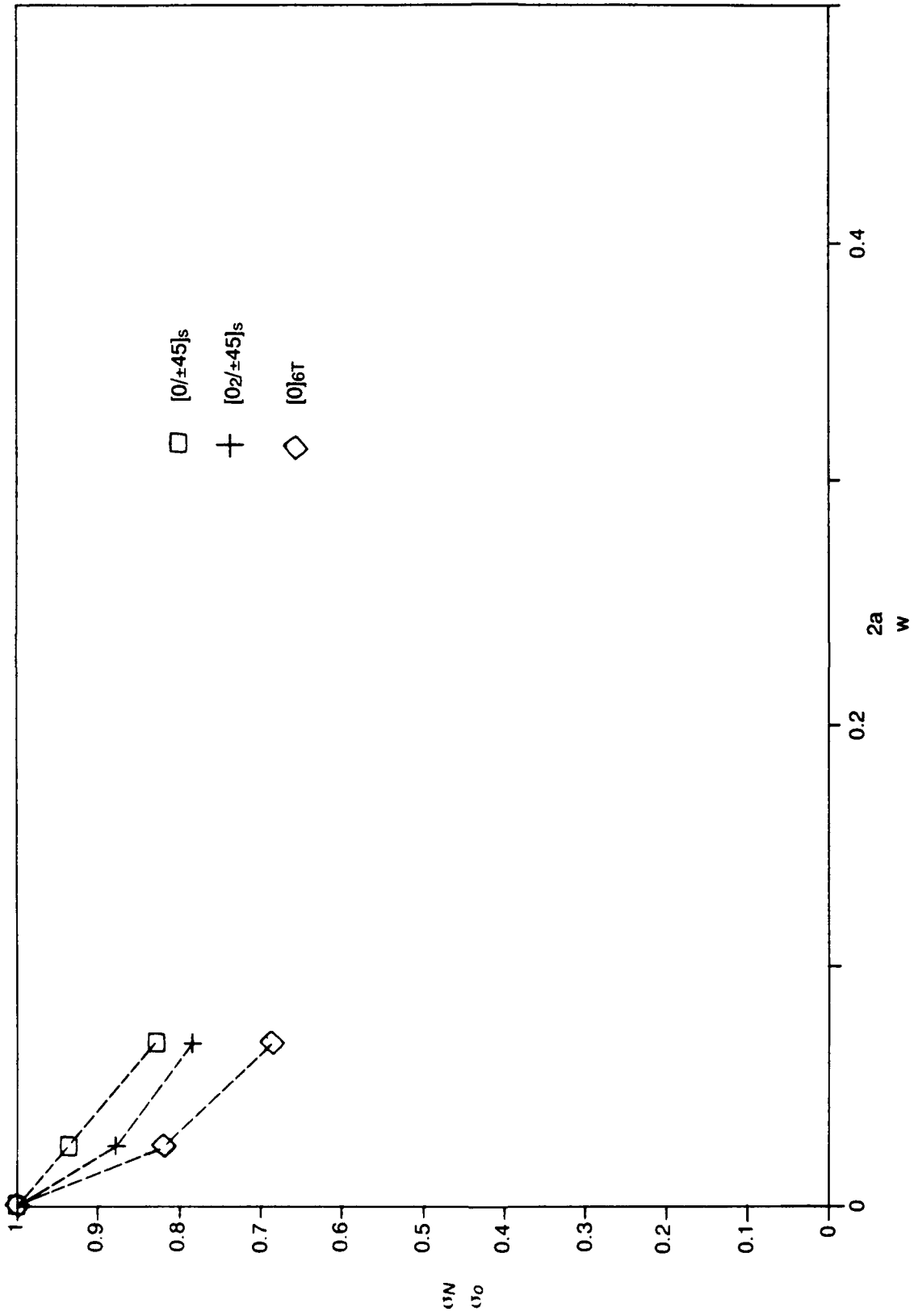


Figure 14. Notch Sensitivities For Various B/AI Laminate Orientations ($w = 19.1\text{mm}$).

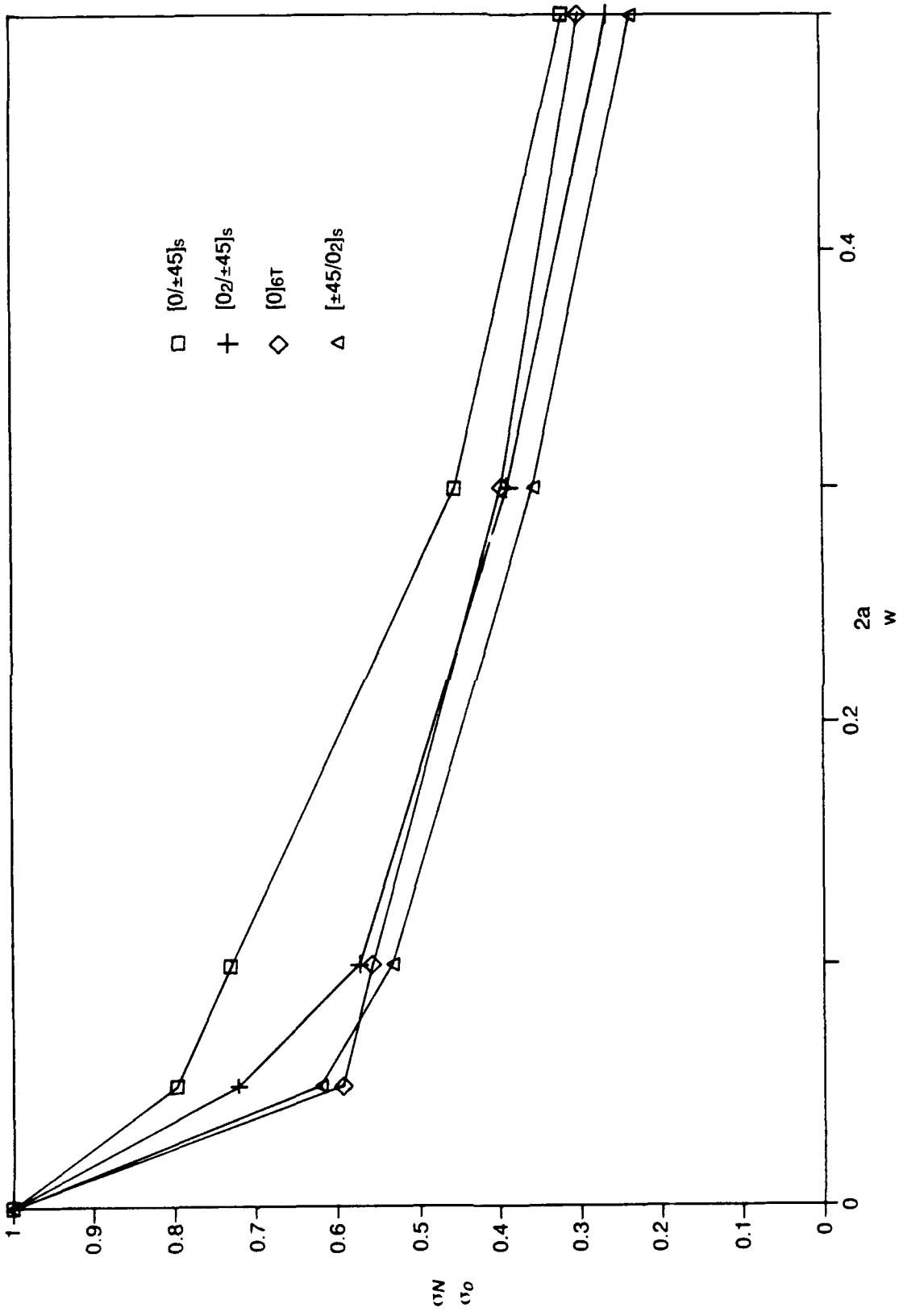


Figure 15. Notch Sensitivities For Various B/AI Laminate Orientations (w = 50.8mm).

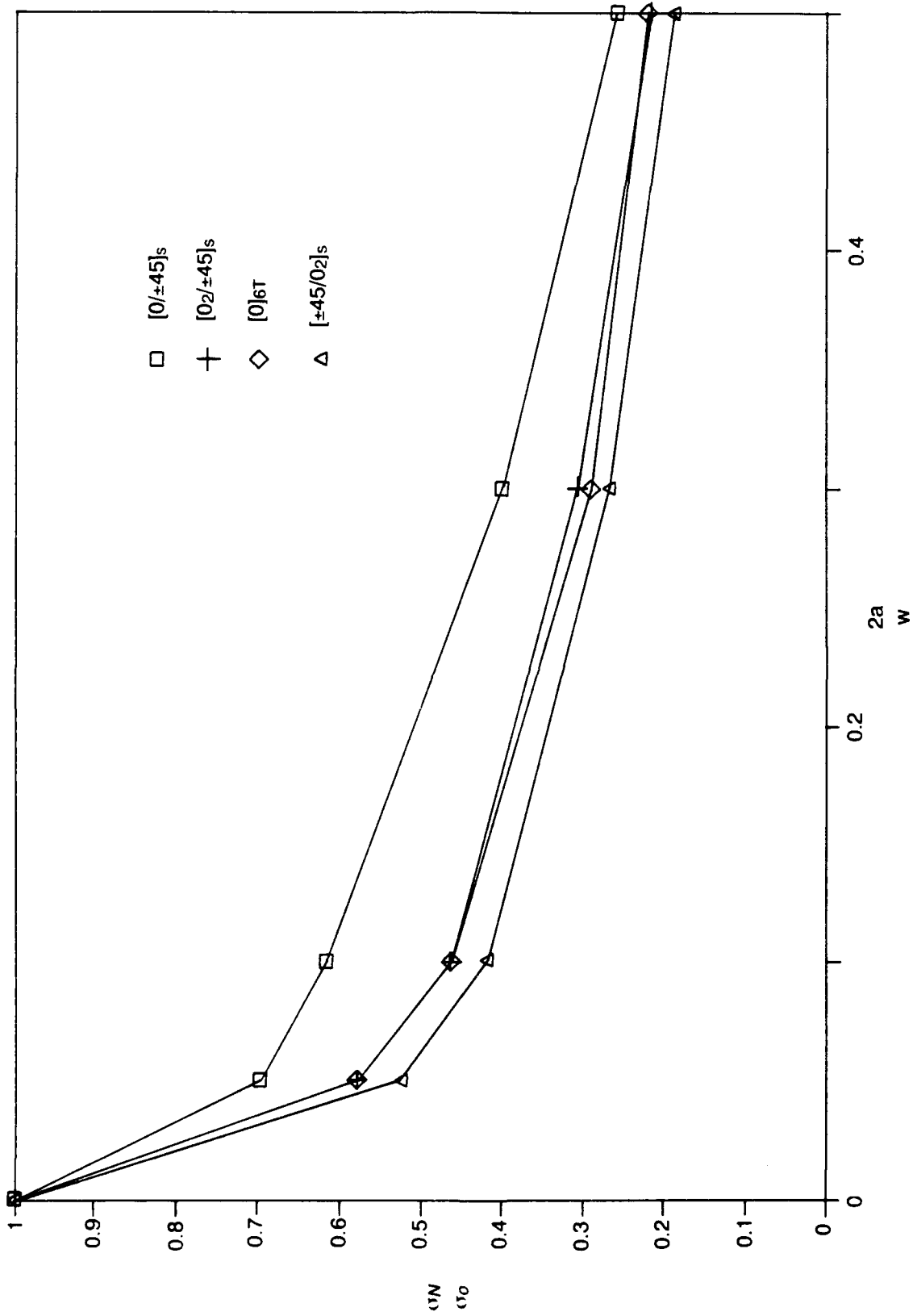


Figure 16. Notch Sensitivities For Various B/Al Laminate Orientations ($w = 101.6\text{mm}$).

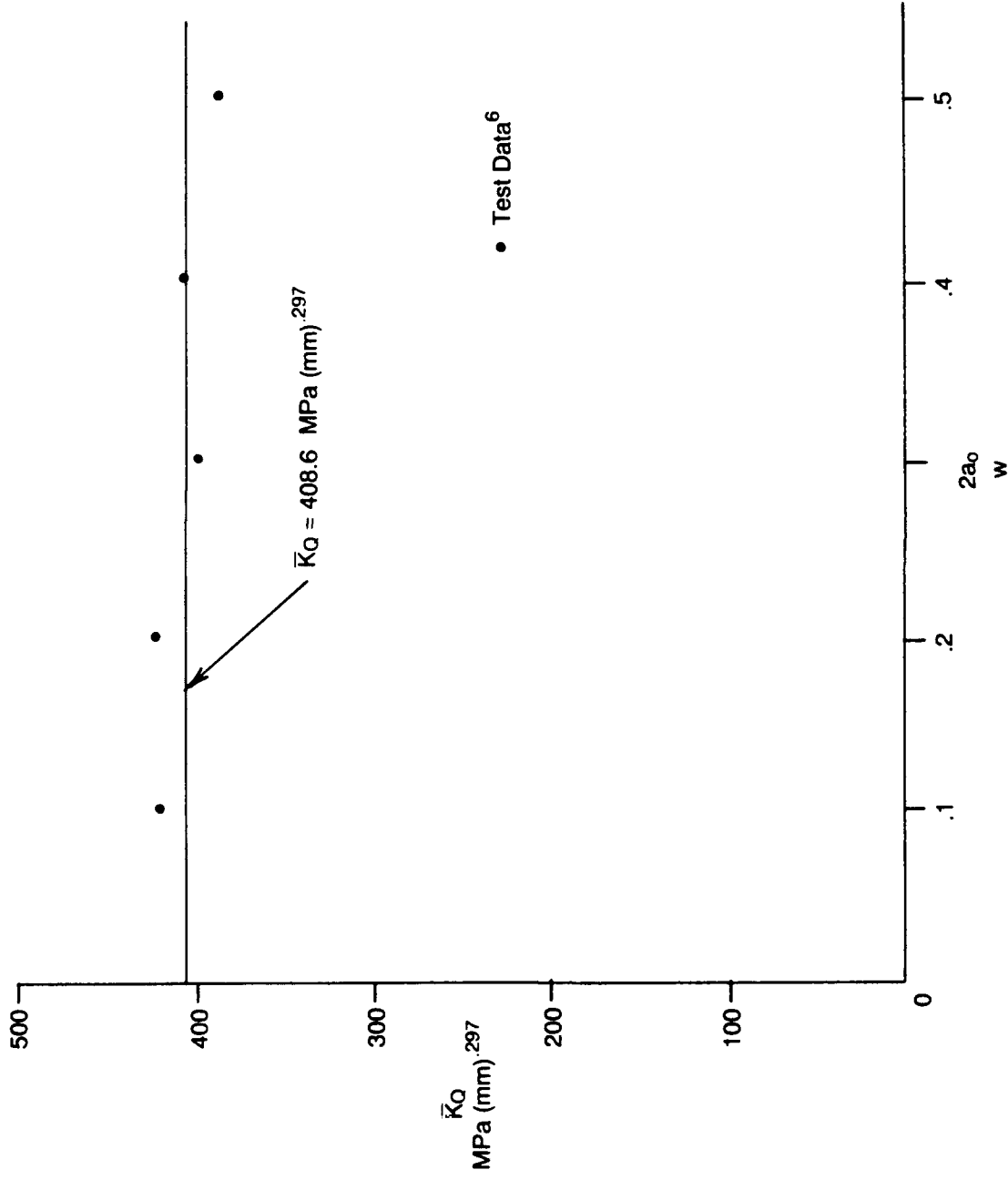


Figure 17. \bar{K}_Q For Gr/Ep With Ply Orientation [0/±45]_{2s}.

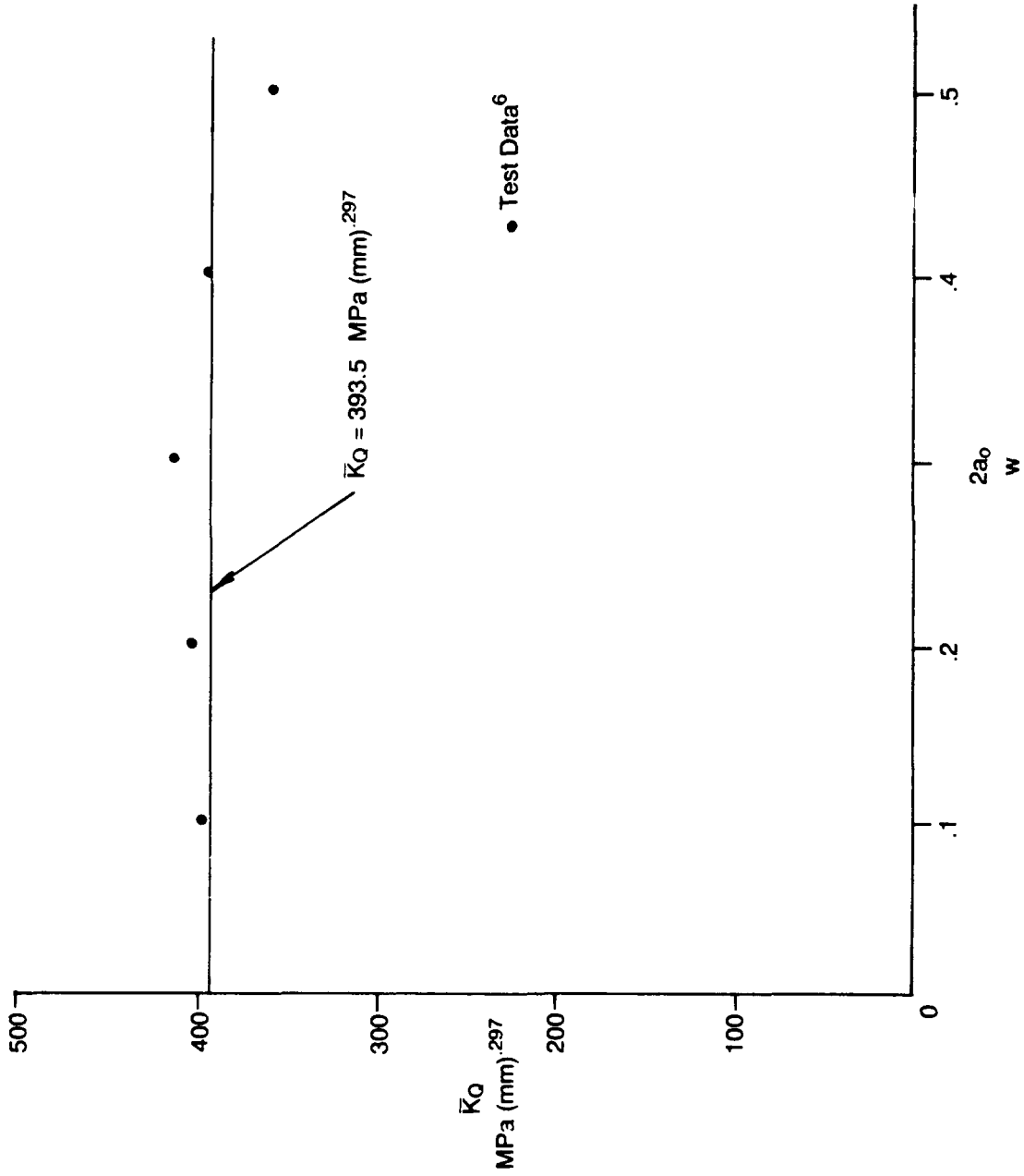


Figure 18. \bar{K}_Q for Gr/Gp With Ply Orientation $[0/\pm 45]_s$.

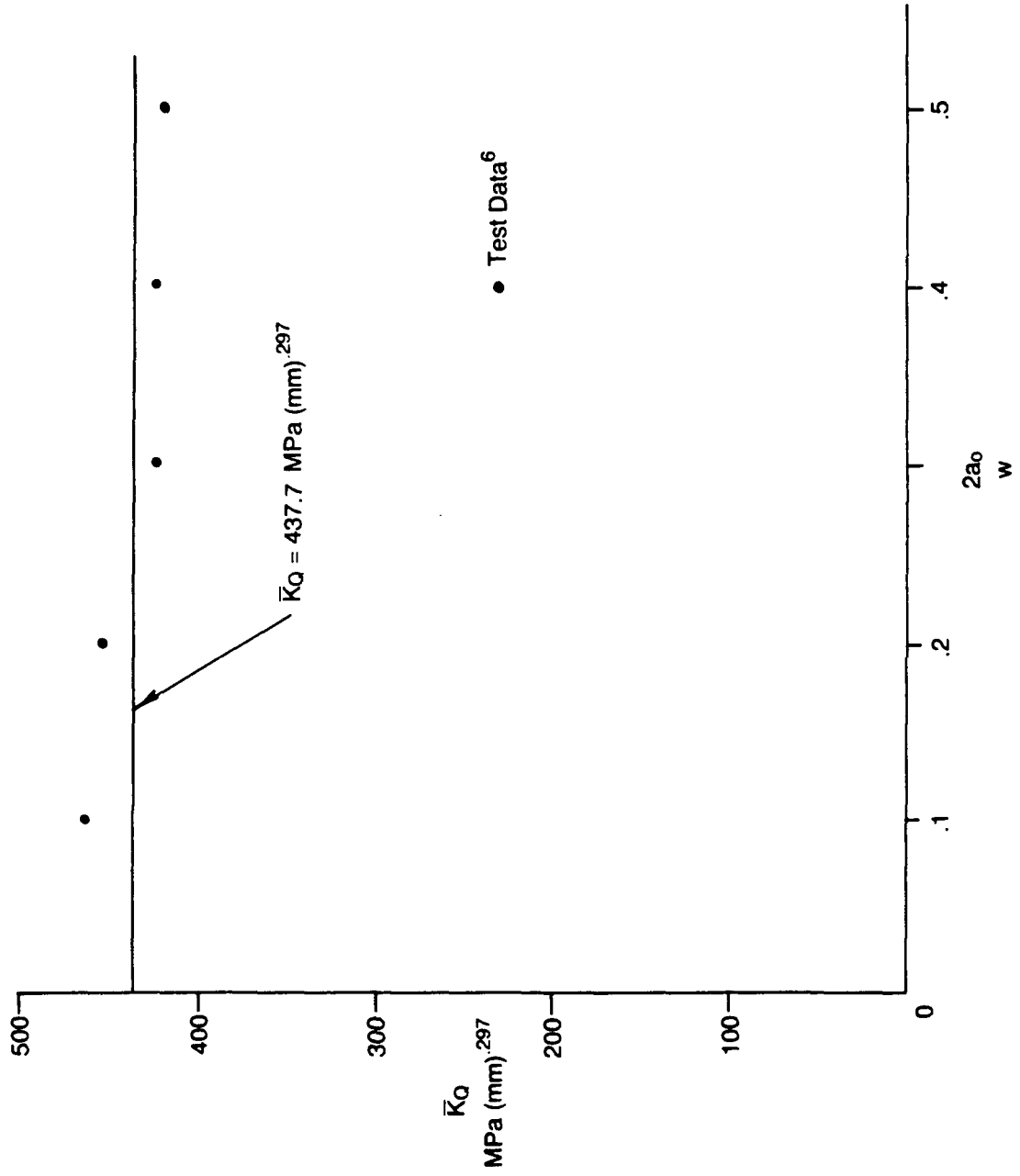


Figure 19. \bar{K}_Q For Gr/Ep With Ply Orientation $[0/90/\pm 45]_s$.

NADC-88118-60

4.2.1 Notched Strength Prediction and Notch Sensitivity

For Gr/Ep composite with center crack, equation (17) becomes

$$\frac{\sigma_N}{\sigma_0} = \frac{1}{Y} \left\{ 1 + \left(\frac{\bar{K}_Q}{\sigma_0} \right)^{-3.367} a_0 \right\}^{-.297} \quad (19)$$

Substituting \bar{K}_Q and σ_0 from Table 8, into equation (19), the fracture strengths of graphite/epoxy for various ply orientations can be obtained and are plotted on Figure 20. The detailed calculations are shown in Appendix B.2. As can be seen from the figure, the correlation between analytical and experimental results is very good.

It can also be seen from Figure 20 that the ratio $\frac{\bar{K}_Q}{\sigma_0}$ (or the inherent flaw size) in Table 8 can be used as a notch sensitivity indicator. The $[0/90/\pm 45]_s$ laminate is less notch sensitive than the $[0/\pm 45]_s$ and $[0/\pm 45]_{2s}$ laminates and accordingly it has a larger ratio of $\frac{\bar{K}_Q}{\sigma_0}$ (or C_0) than the other two laminates.

Table 8. Fracture Parameters For Various Laminate Configurations Of Gr/Ep.

Ply Configuration	σ_o (MPa)	\bar{K}_Q MPa (mm) ^{.297}	$\frac{\bar{K}_Q}{\sigma_o}$ (mm) ^{.297}	C_o (mm)
[0/±45] _{2s}	541.0	408.6	.755	.389
[0/±45] _s	541.0	393.5	.727	.342
[0/90/±45] _s	454.0	437.7	.964	.884

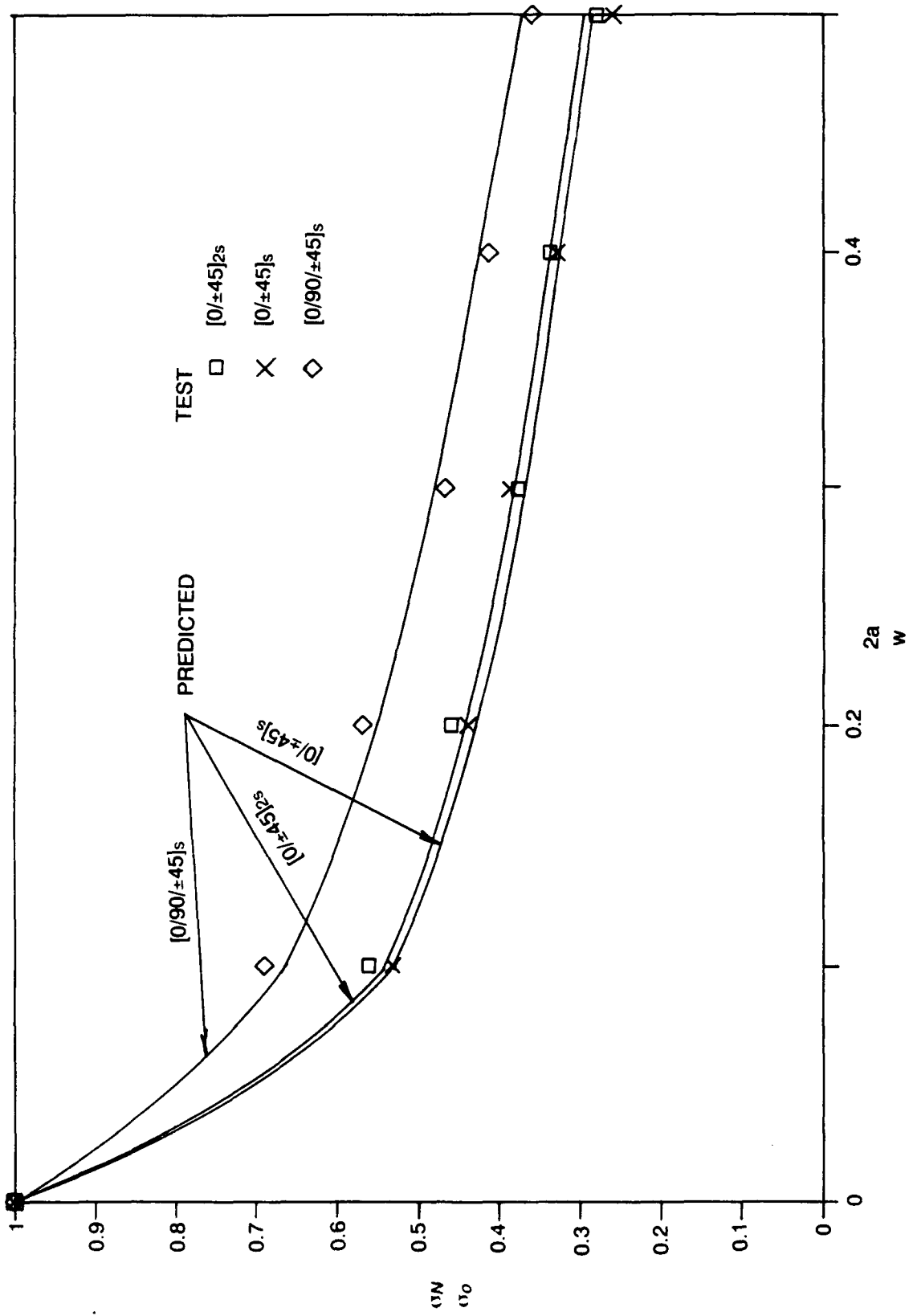


Figure 20. Notch Strength And Notch Sensitivities For Various Gr/Ep Laminate Orientations.

4.3 GLASS/EPOXY (GI/Ep) COMPOSITE

Equation (9) is also used to characterize the \bar{K}_Q for glass/epoxy composites.¹⁶ The detailed calculations are shown in Appendix B.3. \bar{K}_Q for $[0/\pm 45/90]_{2S}$ ply orientation is plotted against $\frac{2a}{w}$ in Figure 21. For GI/Ep composite $m = .289$. As seen in the figure, \bar{K}_Q can be approximately treated as a material constant.

For GI/Ep composites with center crack, equation (17) becomes

$$\frac{\sigma_N}{\sigma_0} = \frac{1}{Y} \left\{ 1 + \left(\frac{\bar{K}_Q}{\sigma_0} \right)^{-3.46} a_0 \right\}^{-.289} \quad (20)$$

with

$$\bar{K}_Q = 274 \text{ MPa (mm)}^{.289}$$

$$\sigma_0 = 320 \text{ MPa}$$

Equation (20) becomes

$$\frac{\sigma_N}{\sigma_0} = \frac{1}{Y} \{ 1 + 1.7108 a_0 \}^{-.289} \quad (21)$$

For the laminate with a center crack⁸,

$$Y = \sqrt{\sec\left(\frac{\pi a_0}{w}\right)} \quad (22)$$

where a_0 = half crack length.

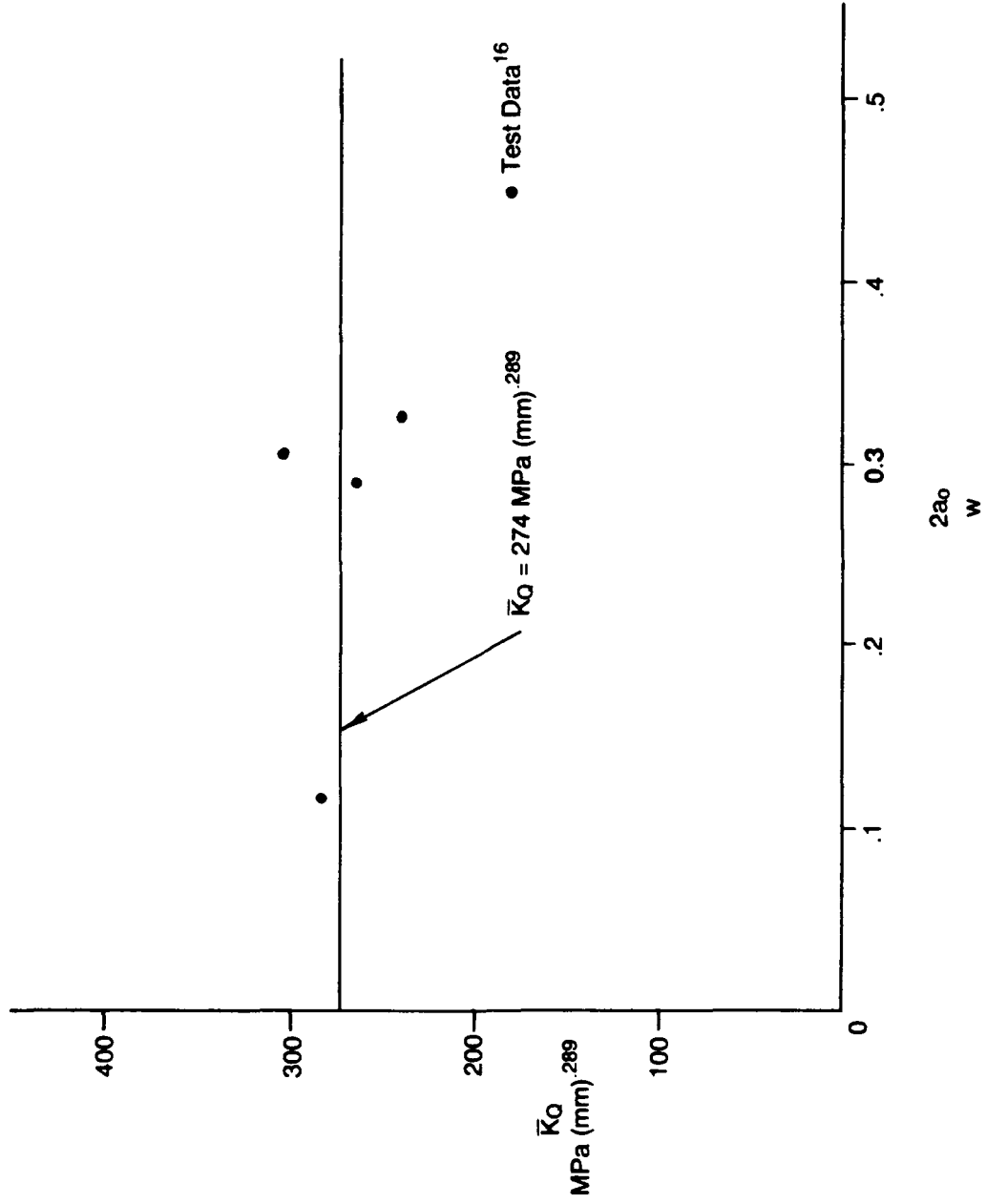


Figure 21. \bar{K}_Q for GI/Ep with Ply Orientation $[0/\pm 45/90]_{2s}$.

NADC-88118-60

For the laminate with a center hole. Y is assumed in the following form

$$Y = \sqrt{\sec\left(\frac{\pi R_o}{w}\right)} \quad (23)$$

where R_o = radius of the hole

Equation (21) was plotted for $G/E_p [0/\pm 45/90]_{2s}$ laminates with a center crack and a hole as shown in Figure 22.

It can be seen that the correlations between analytical results and test results are good. Also, note that a center hole decreases the fracture strength of a composite laminate slightly more than a center crack does.

4.4 COMPARISON OF ANALYTICAL RESULTS BETWEEN ANISOTROPIC AND MICROSCOPIC MODELS

Composite materials made by combining two materials with different elastic moduli are by nature anisotropic in the gross sense. The anisotropic model for composite materials is to assume that the composite is a homogeneous, anisotropic solid. For an anisotropic fracture $m = .5$.¹⁷ Applying the inherent flaw concept for an anisotropic model, for center crack specimen, we have

$$K_Q = Y \sigma_N (a_0 + C_0^*)^{1/2} \quad (24)$$

$$K_Q = \sigma_0 (C_0^*)^{1/2} \quad (25)$$

Note that K_Q has dimensions different from those of \bar{K}_Q and C_0^* is the inherent flaw size corresponding to an anisotropic model.

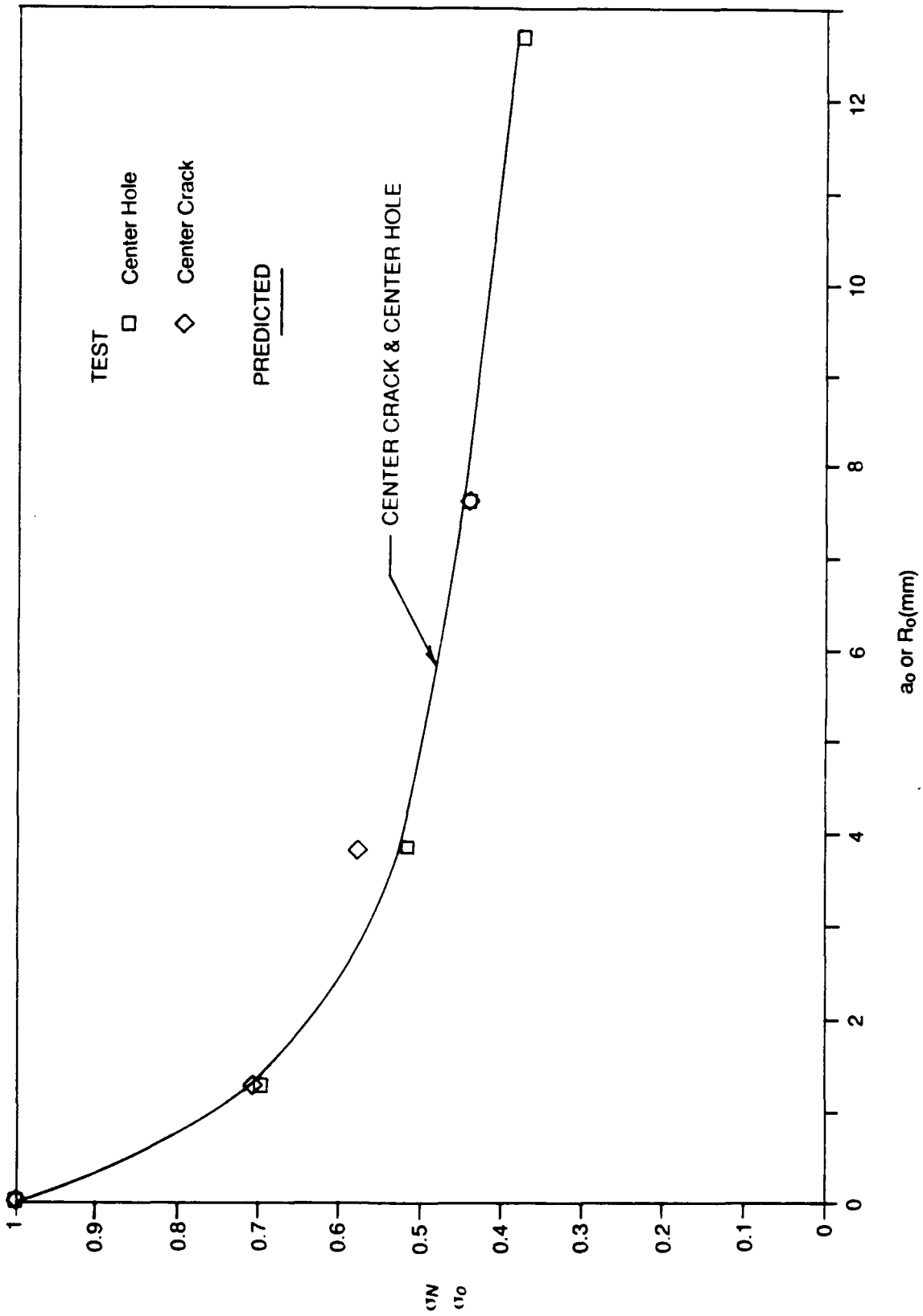


Figure 22. Fracture Strength Prediction For GI/Ep [0/±45/90]_{2s}.

NADC-88118-60

Examining equations (24) and (25), we can derive the following useful equations for an anisotropic model

$$C_0^* = \frac{a_0}{\left(\frac{\sigma_0}{Y\sigma_N}\right)^2 - 1} \quad (26)$$

$$\frac{\sigma_N}{\sigma_0} = \frac{1}{Y} \left(\frac{C_0^*}{a_0 + C_0^*} \right)^{1/2} \quad (27)$$

$$K_Q = \sigma_0 (a_0)^{1/2} \left\{ \left(\frac{Y\sigma_N}{\sigma_0} \right)^{-2.0} - 1 \right\}^{-.5} \quad (28)$$

Equation (26) can be used to obtain C_0^* through the least square fit method. It has been determined for the anisotropic model that C_0^* found by the least square fit method predicts the test data better than C_0^* found by the average equivalent stress intensity method. Equation (27) can be used to predict the fracture strength of composite laminates.

In this report, only B/AI composites will be used to demonstrate the superiority of the microscopic model over the anisotropic model.

Tables 9 to 12 show the comparison of analytical results between the microscopic and anisotropic models. These results are also plotted on Figures 23 to 26. It is clear that the microscopic model predicts better results than the anisotropic model. Note that the results of the *microscopic model* are copied from Tables 1 to 4, while the results of the anisotropic model are shown in Appendix C.

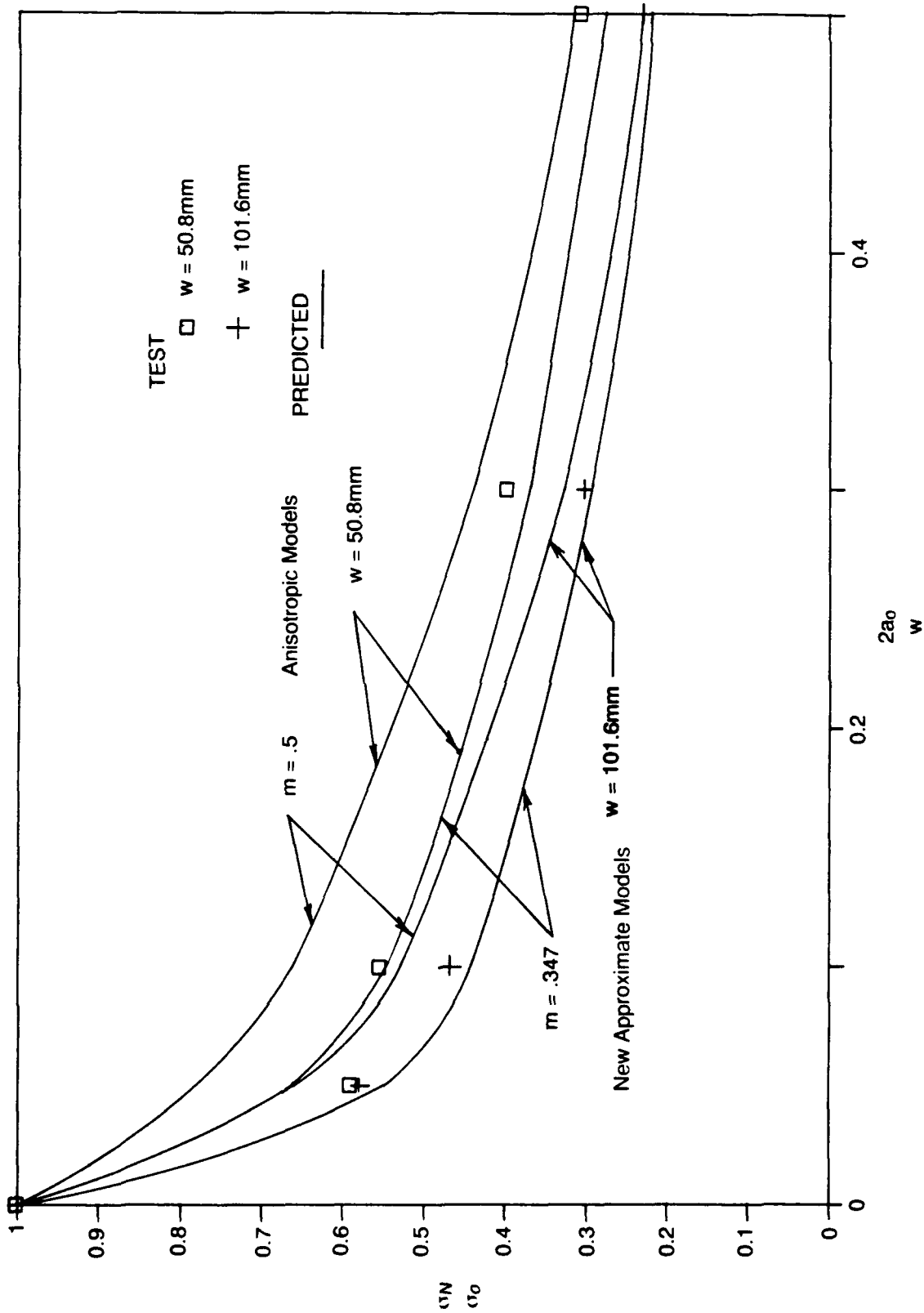


Figure 23. Comparison Of Analytical Results Between Anisotropic And New Approximate Models $B/AI(0)_{\text{EST}}$.

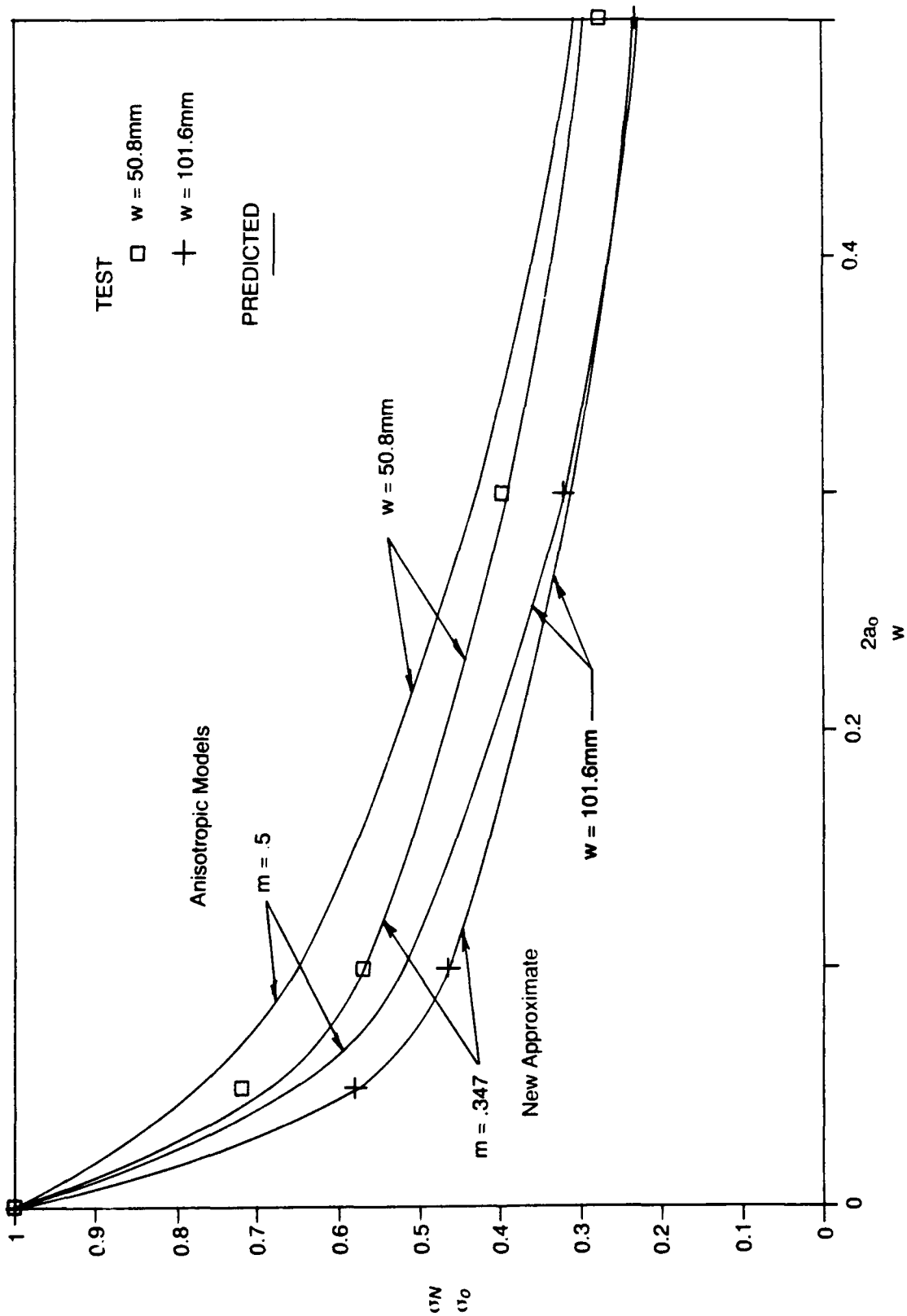


Figure 24. Comparison Of Analytical Results Between Anisotropic And New Approximate Models $B/AI (0_2 \pm 45)_s$.

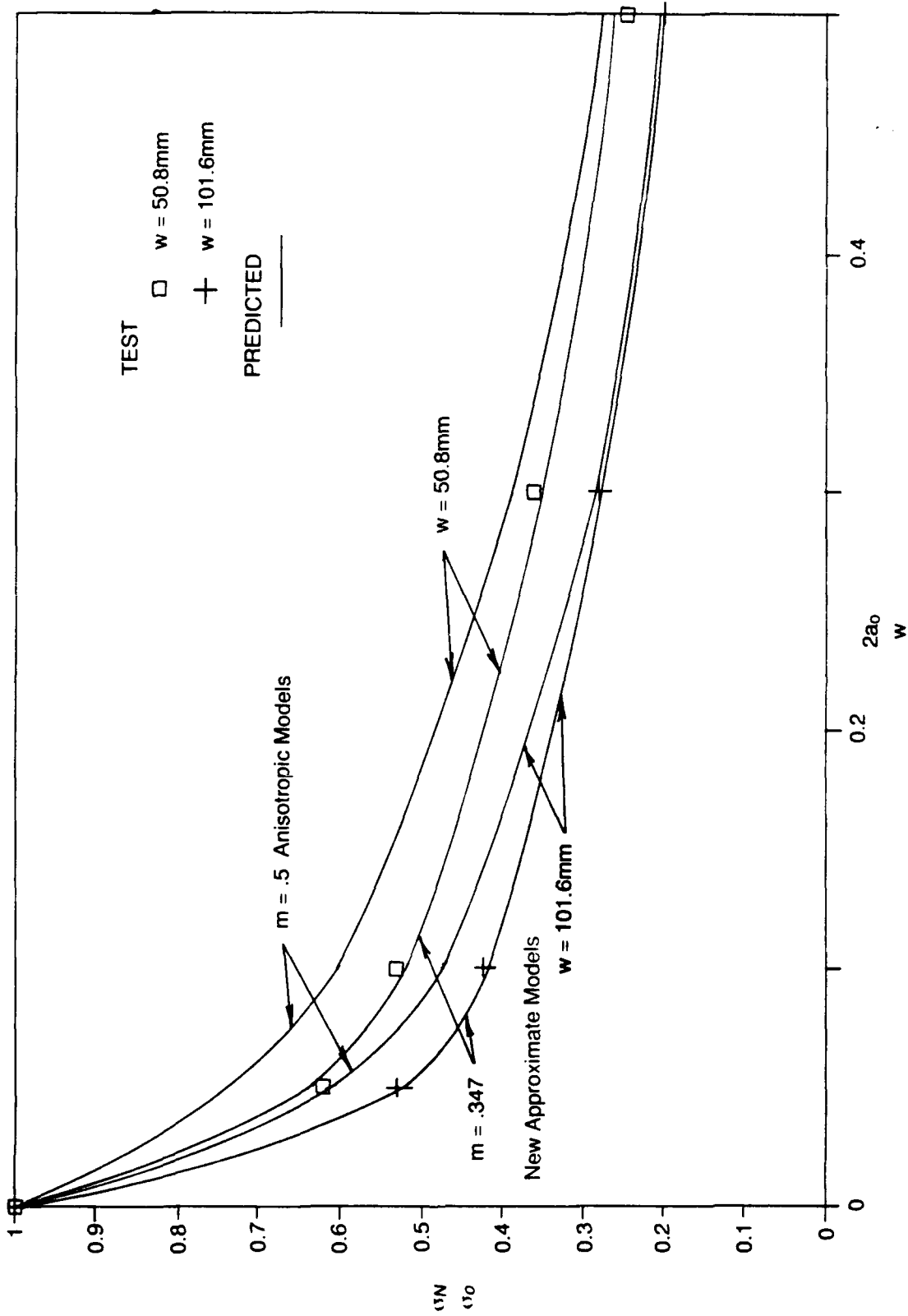


Figure 25. Comparison Of Analytical Results Between Anisotropic And New Approximate Models $B/AI (+45/0)_s$.

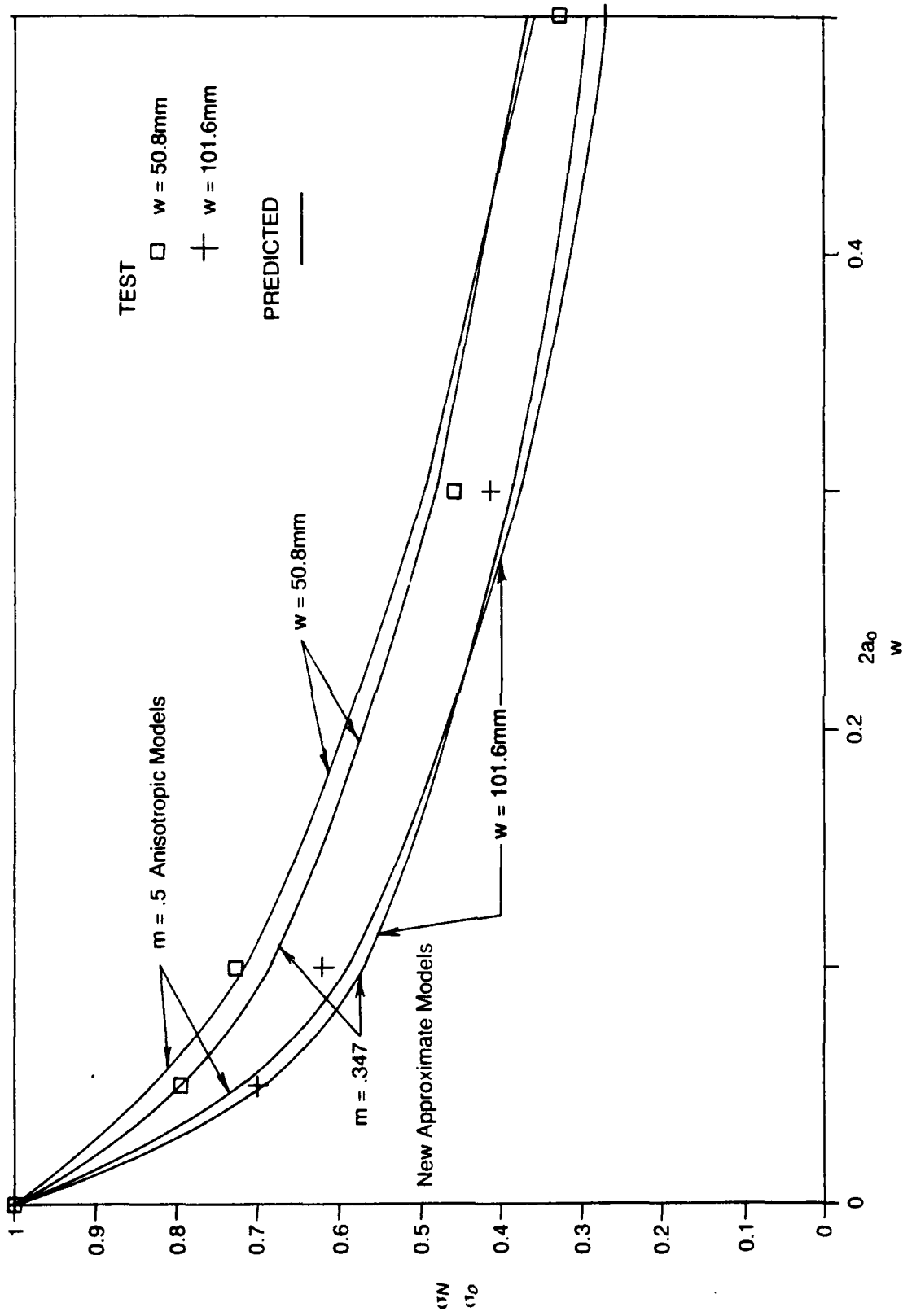


Figure 26. Comparison Of Analytical Results Between Anisotropic And New Approximate Models B/AI (0/±45)_s.

Table 9. Comparison Of Analytical Results Between Anisotropic And New Approximate Models B/AI [0]_{6T}.

a_0 (mm)	$\frac{2a_0}{w}$	$\left(\frac{\sigma_N}{\sigma_0}\right)_{Test}$	Microscopic Model ($m = .347$)	Anisotropic Model ($m = .5$)
0.25	.03	.818	.878	.942
.65	.07	.6845	.760	.866
1.25	.05	.592	.663	.786
2.55	.05	.580	.549	.666
2.55	0.10	.555	.546	.663
5.10	0.1	.468	.443	.532
7.60	0.3	.4003	.371	.44
12.7	0.5	.3098	.279	.317
15.25	0.3	.3024	.295	.329
25.40	0.5	.232	.221	.233

Table 10. Comparison Of Analytical Results Between Anisotropic And New Approximate Models B/AI [$0_2/\pm 45$]._s

a_0 (mm)	$2a_0$ w	$\left(\frac{0M}{\sigma_0}\right)_{Test}$	Microscopic Model ($m = .347$)	Anisotropic Model ($m = .5$)
0.25	.03	.878	.891	.938
.65	.07	.782	.782	.858
1.25	.05	.721	.686	.775
2.55	.05	.579	.572	.653
2.55	0.10	.571	.570	.649
5.10	0.1	.464	.464	.518
7.6	0.3	.395	.389	.427
12.7	0.5	.274	.293	.307
15.25	0.3	.321	.310	.318
25.40	0.5	.229	.232	.225

Table 11. Comparison Of Analytical Results Between Anisotropic And New Approximate Models B/AI [$\pm 45/0_2$].s.

a_0 (mm)	$2a_0$ w	$\left(\frac{\sigma_{11}}{\sigma_0}\right)_{Test}$	Microscopic Model (m = .347)	Anisotropic Model (m = .5)
0.25	.03	---	---	---
.65	.07	---	---	---
1.25	.05	.619	.633	.735
2.55	.05	.528	.520	.606
2.55	0.10	.531	.517	.602
5.10	0.1	.423	.417	.472
7.6	0.3	.361	.349	.386
12.7	0.5	.245	.262	.275
15.25	0.3	.281	.276	.284
25.40	0.5	.201	.207	.200

Table 12. Comparison Of Analytical Results Between Anisotropic And New Approximate Models B/AI [0/±45]_s.

a_0 (mm)	$\frac{2a_0}{W}$	$\left(\frac{\sigma_N}{\sigma_0}\right)_{Test}$	Microscopic Model ($m = .347$)	Anisotropic Model ($m = .5$)
0.25	.03	—	—	—
0.65	.07	.828	.865	.895
1.25	.05	.796	.789	.828
2.55	.05	.699	.692	.721
2.55	0.10	.730	.688	.717
5.10	0.1	.620	.569	.591
7.6	0.3	.458	.481	.495
12.7	0.5	.329	.367	.361
15.25	0.3	.413	.388	.376
25.40	0.5	.271	.293	.268

5.0 CONCLUSIONS AND RECOMMENDATIONS

5.1 CONCLUSIONS

- The methodology developed here can be used to characterize the fracture toughness of the composite laminates and can be used as a design tool to predict the fracture strength of various composite laminates.
- The parameter \bar{K}_Q which was called critical equivalent stress intensity factor is defined, and can be treated as a material constant for composite laminate.
- The new approximate model provides better results than those of the anisotropic model.
- The larger the ratio $\frac{\bar{K}_Q}{\sigma_0}$ (or the inherent flaw size, C_0), the higher the damage tolerance.

5.2 RECOMMENDATIONS

- Further verification of microscopic theory with test results of various composites materials is needed.
- Apply the theory developed here to predict the fracture strength of composite laminates with various crack angles.
- Develop a methodology to predict the inherent flaw size at the crack tip before fracture.

NADC-88118-60

THIS PAGE INTENTIONALLY LEFT BLANK

NADC-88118-60

6.0 REFERENCES

1. Adams, D. F. and Mahishi, J.M. "Delamination Micromechanics Analysis", NASA Report, N85-31237, May 1985.
2. Whitney, J.M., "Fracture Analysis of Laminates", Composites Engineered Materials Handbook, ASM International, Volume 1, 1987.
3. Waddoups, M.G., Eisenmann, J.R. and Kaminski, B.E., "Microscopic Fracture Mechanics of Advanced Composites Materials", Journal of Composite Material, Vol. 5, 1971, p.446.
4. Bowie, O.L., "Analysis of an Infinite Plate Containing Radial Cracks Originating from the Boundary of an Internal Circular Hole", Journal of Mathematics and Physics, Vol. 35, 1956, p.60.
5. Adsit, N.R. and Waszczak, J.P. "Fracture Mechanics Correlation of Boron/Aluminum Coupon Containing Stress Risers", ASTM STP 593, 1975.
6. Morris, D.H. and Han, H.T., "Fracture Resistance Characterization of Graphite/Epoxy Composites", Composites Materials: Testing and Design, ASTM, STP 617, pp.5-17, 1976
7. Awerbuch, J., and Han, H.T., "Crack Tip Damage and Fracture Toughness of Boron/Aluminum Composites", Journal of Composite Materials, Vol. 13, April 1979, pp. 82-1078.
8. Poe, C.C.Jr., and Sova, J.A. "Fracture Toughness of Boron/Aluminum Laminates with Various Proportions of 0° and ±45° Plies", NASA TP 1707, 1980.
9. Mar, J.W. and Lin, D.Y., "Fracture Mechanics Correlation for Tensile Failure of Filamentary Composites with Holes", Journal of Aircraft, Vol. 14, p. 703, 1977.
10. Lin, K.Y. and Mar, J.W., "Finite Element Analysis of Stress Intensity factors for Cracks at a Bi-Material Interface", International Journal of Fracture, 12, pp. 521-531, 1976.
11. Bogy, D.B., "On the Plane Elastostatic Problem of a Loaded Crack Terminating at a Material Interface", Journal of Applied Mechanics, Transaction ASME, 38, Series E., No. 4 PP. 911-918, December 1971.
12. Zak, A.R. and Williams, M.L., Journal of Applied Mechanics, 30 Transaction of ASME, 85, Series E. pp. 142-143, March 1963.
13. Irwin G.R. "Analysis of Stresses and Strains Near the end of a crack Traversing a Plate", Journal of Applied Mechanics, Transactions ASME, Vol. 24, 1957
14. Johnson, W.S. and Bigelow, C.A., "Experimental and Analytical Investigation of Fracture Process of Boron/Aluminum Laminates Containing Notches", NASA TP 2187, 1983.
15. Mardell, J.F.Wang, Su-Su, McGaury, J. Frederich, "The Extension of Crack Tip Damage Zones in Fiber Reinforced Plastic Laminates", Journal of Composite Materials, Vol. 9, July 1975.

NADC-88118-60

16. Nuismer, R.J. and Whitney, J.M., "Uniaxial Failure, of Composite Laminates Containing Stress Concentrations", *Fracture Mechanics of Composites*, ASTM STP 593, American Society for Testing and Materials, Philadelphia, pp. 117-142, 1975.

17. Wu, E.M., "Strength and Fracture of Composites", *Fracture and Fatigue, Composite Materials*, Vol. 5, 1974.

18. Goree, J.G. and Dharani, R. "Mathematical Modeling of Damage in Unidirectional Composites". NASA Contractor Report 3453, 1981.

19. Mar, J.W. and Lin, K.Y., "Fracture of Boron/Aluminum Composites with Discontinuities", *Journal of Composite Materials*, Vol. 11, Oct. 1977, pp. 405-421.

NADC-88118-60

APPENDIX A

**CALCULATION OF THE ORDER OF STRESS
SINGULARITY AT A BI-MATERIAL INTERFACE**

NADC-88118-60

APPENDIX A

CALCULATION OF THE ORDER OF STRESS SINGULARITY AT A BI-MATERIAL INTERFACE

In the case of a crack, normal to the bi-material interface as shown in figure A-1, the characteristic equation to determine the order of stress singularity is given as follows.¹⁰:

$$\tau^2(-4\alpha^2 + 4\alpha\beta) + 2\alpha^2 - 2\alpha\beta + 2\alpha - \beta + 1 + (-2\alpha^2 + 2\alpha\beta - 2\alpha + 2\beta) \cos \tau \pi = 0 \quad (\text{A-1})$$

where

$$\alpha = \frac{\frac{\mu_1}{\mu_2} - 1}{\eta_1 + 1}$$

$$\beta = \frac{\mu_1 (\eta_2 + 1)}{\mu_2 (\eta_1 + 1)} \quad (\text{A-2})$$

$\eta_1 = 3 - 4\nu_1$, $\eta_2 = 3 - 4\nu_2$ for plane strain

$\eta_1 = (3 - \nu_2)/(1 + \nu_1)$, $\eta_2 = (3 - \nu_2)/(1 + \nu_2)$ for plane stress

μ_1, μ_2 = Shear modulus of medium 1 and 2 respectively

ν_1, ν_2 = Poison's ratio for medium 1 and 2 respectively

The stresses near the crack tip (for $\theta = 0$) can be written as

$$\sigma_x \sim r^{\tau-1}$$

$$\sigma_y \sim r^{\tau-1}$$

$$\tau_{xy} \sim r^{\tau-1} \quad (\text{A-3})$$

The order of stress singularity is defined as

$$m = 1 - \tau \quad (\text{A-4})$$

By treating the matrix as medium 1, and fiber as medium 2, equations (A-1) to (A-4) are used to calculate the order of singularities for various composite materials as follows:

BORON/ALUMINUM

The properties of boron fiber and aluminum matrix are as follows:

Aluminum: $\mu_1 = 3.76$ msi, $\nu_1 = .33$

Boron: $\mu_2 = 26.77$ msi, $\nu_2 = .13$

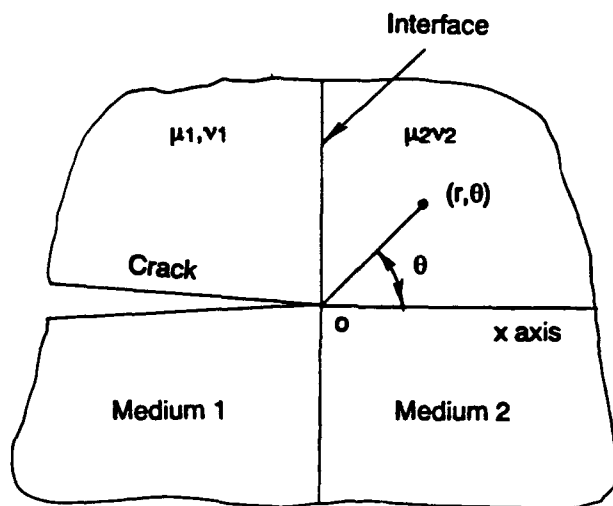


Figure A-1. Crack Normal To The Bi-Material Interface.

Substituting these properties into equations (A-1) and (A-2) for plane stress case, we have the following characteristic equation:

$$.5191 \tau^2 - .6448 \cos \tau \pi - .5204 = 0 \quad (A-5)$$

Solving equation (A-5), we have

$$\tau = .653$$

From equation (A-4)

$$m = .347$$

GRAPHITE/EPOXY

For Thornel graphite fiber properties

$$\mu_2 = 4 \text{ msi} \quad \nu_2 = .2$$

For Epoxy matrix properties

$$\mu_1 = .19 \text{ msi} \quad \nu_1 = .35$$

Applying the same procedures as for the Boron/Aluminum Composite, we find

$$m = .297 \text{ for Thornel Graphite/Epoxy}$$

NADC-88118-60

GLASS/EPOXY

For E-type glass fiber,

$$\mu_2 = 4.4 \text{ msi} \quad \nu_2 = .2$$

For Epoxy matrix,

$$\mu_1 = .17 \text{ msi} \quad \nu_1 = .35$$

Applying the same procedure as for the Boron/Aluminum composite we find:

$$m = .289 \text{ for E-type Glass/Epoxy}$$

NADC-88118-60

THIS PAGE INTENTIONALLY LEFT BLANK

NADC-88118-60

APPENDIX B
CALCULATION OF \bar{K}_Q AND $\frac{\sigma_N}{\sigma_0}$
FOR VARIOUS COMPOSITE LAMINATES

NADC-88118-60

APPENDIX B

CALCULATION OF \bar{K}_Q AND $\frac{\sigma_N}{\sigma_0}$ FOR VARIOUS COMPOSITE LAMINATES

The following equations were used to calculate \bar{K} and $\frac{\sigma_N}{\sigma_0}$

$$\bar{K} = a_0^m \sigma_0 \left\{ \left(\frac{Y \sigma_N}{\sigma_0} \right)^{-1/m} - 1 \right\}^{-m} \quad (B-1)$$

$$\frac{\sigma_N}{\sigma_0} = \frac{1}{Y} \left\{ \frac{1}{1 + \left(\frac{\bar{K}}{\sigma_0} \right)^{-1/m} a_0} \right\}^m \quad (B-2)$$

B.1 BORON/ALUMINUM COMPOSITE (M = .347)

B.1.1 Determination of \bar{K}_Q (Tables 1 to 4)

Column 5 of Tables 1 to 4 listed the test results of $\frac{\sigma_N}{\sigma_0}$. Substituting these quantities into equation (B-1), we obtain \bar{K} for various ξ (i.e. $\frac{2a_0}{w}$) values as shown in Column 6 of Tables 1 to 4. \bar{K}_Q is then defined as

$$\bar{K}_Q = \bar{K}_{AVG} = \frac{1}{n} \sum_{i=1}^n \bar{K}_i \quad (B-3)$$

Where n = total number of test data, and where \bar{K}_{AVG} rather than \bar{K}_{LSF} is chosen to be \bar{K}_Q , the critical stress intensity factor as demonstrated in Figures 3 through 6 in Section 3.2.

B.1.2 Determination Of \bar{K}_Q From Test Data Of Reference 5

Column 4 of Tables B-1 to B-3 shows the test results for various ratios of ξ . Using the same procedures described in the previous section we can obtain \bar{K}_Q for composite laminates with a center hole, double edge notch, and center slit respectively as shown in Column 5 of Table B-1 to Table B-3.

Table B-1. Unidirectional B/Al Composite Laminates With Center Hole.

$$\sigma_0 = 1470.79 \text{ MPa}$$

R _o (mm)	ξ	Y _H	$\left(\frac{\sigma_N}{\sigma_0} \right)_{\text{TEST}}$	K̄ MPa (mm) ^{.347}	$\frac{\sigma_N}{\sigma_0}$
1.5875	.25	1.04	.542	1048.31	.601
2.38125	.25	1.04	.521	1149.86	.538
3.175	.25	1.04	.513	1247.19	.495
6.35	.25	1.04	.443	1339.3	.400

$$\bar{K}_Q = \bar{K}_{AVG} = 1196 \text{ MPa (mm)}^{.347}$$

$$Y_H = \sqrt{\sec\left(\frac{\pi \xi}{2}\right)}$$

NADC-88118-60

Table B-2. Unidirectional B/AI Composite Laminates With Double Edge Notch.

a _o (mm)	ξ	Y _c Y _o	$\left(\frac{\sigma_N}{\sigma_o}\right)_{TEST}$	\bar{K} MPa(mm) ^{.343}	$\frac{\sigma_N}{\sigma_o}$
1.905	.3	1.01	.565	1270.02	.546
2.8575	.3	1.01	.453	1128.47	.489
3.81	.3	1.01	.471	1302.47	.443
7.62	.3	1.01	.338	1156.97	.354

$$K_Q = K_{AVG} = 1214.5 \text{ MPa (mm)}^{.347}$$

$$Y_c = (1.98 + .36 \xi - 2.12 \xi^2 + 3.42 \xi^3)/1.77$$

Table B-3. Unidirectional B/AI Composite Laminates With Center Slit.

a _o (mm)	ξ	Y _H	$\left(\frac{\sigma_N}{\sigma_o}\right)_{TEST}$	\bar{K} MPa (mm) ^{.347}	$\frac{\sigma_N}{\sigma_o}$
3.81	.4	1.11	.431	1160.85	.454
7.62	.4	1.11	.382	1292.61	.362

$$\bar{K}_Q = \bar{K}_{AVG} = 1227 \text{ MPa (mm)}^{.347}$$

$$Y_c = \sqrt{\sec\left(\frac{\pi \xi}{2}\right)}$$

Table B-4. Fracture Strength Prediction For B/AI [0]_{6T} With Center Hole.

R _o (mm)	ξ	Y _H	\bar{K}_Q .347 MPa(mm)	$\left(\frac{\sigma_N}{\sigma_o}\right)_T$	$\left(\frac{\sigma_N}{\sigma_o}\right)$	Error %
1.59	.0625	1.0	1360	.628	.625	-0.5
3.175	.125	1.01	1360	.538	.510	-5.0
6.35	.125	1.01	1360	.419	.412	-1.7
6.35	.25	1.04	1360	.371	.4	7.9
12.7	.25	1.04	1360	.299	.319	6.7

$$\frac{\sigma_N}{\sigma_o} = \frac{1}{Y} (1 + 1.813R_o)^{-.347}$$

NADC-88118-60

B.1.3 Prediction of $\frac{\sigma_N}{\sigma_0}$ for Boron/Aluminum Laminates with Center Hole

From Tables 1 to Table 4, we have \bar{K}_Q for $[0]_{6T}$, $[0_2/\pm 45]_s$ and $[0/\pm 45]_s$ as $1360 \text{ MPa (mm)}^{.347}$, $685.6 \text{ MPa (mm)}^{.347}$ and $633.5 \text{ MPa (mm)}^{.347}$ respectively. Substituting these quantities into equation (B-2) for \bar{K} , we can predict the fracture strength of composite laminates with a center hole as shown in Tables B-4 to B-6. The test data are obtained from Reference 14.

Table B-5. Fracture Strength Prediction For B/Al $[0_2/\pm 45]_s$ With Center Hole.

R_0 (mm)	ξ	Y_H	\bar{K}_Q	$\left(\frac{\sigma_N}{\sigma_0}\right)_T$	$\left(\frac{\sigma_N}{\sigma_0}\right)$	Error %
1.59	.0625	1.0	685.6	.625	.649	3.8
3.175	.125	1.01	685.6	.525	.533	1.5
16.35	.125	1.01	685.6	.475	.432	-9.2
6.35	.25	1.04	685.6	.450	.420	-6.7
12.7	.25	1.04	685.6	.375	.335	10.0

$$\frac{\sigma_N}{\sigma_0} = \frac{(1 + 1.56R_0)^{-.347}}{Y_H}$$

Table B-6. Fracture Strength Prediction For B/Al $[0/\pm 45]_s$.

a_0 (mm)	ξ	Y_H	\bar{K}_Q	$\left(\frac{\sigma_N}{\sigma_0}\right)_T$	$\left(\frac{\sigma_N}{\sigma_0}\right)$	Error %
1.59	.0625	1.0	633.5	.792	.756	-4.6
3.175	.125	1.01	633.5	.645	.642	0.
6.35	.125	1.01	633.5	.585	.533	-9.0
6.35	.25	1.04	633.5	.499	.517	3.5
12.7	.25	1.04	633.5	.465	.419	-10.0

$$\frac{\sigma_N}{\sigma_0} = \frac{1}{Y} (1 + .781R_0)^{-.347}$$

NADC-88118-60

B.2 GRAPHITE/EPOXY COMPOSITE (m=.297)

Substituting m=.297 and the test data from Reference 6 as shown in Column 4 of Tables B-7 to B-9, into equation (B.1), we can obtain \bar{K} as listed on Column 5 of the Tables. Then use equation (B-3) to obtain \bar{K}_Q .

After obtaining \bar{K}_Q , substituting these quantities into equation (B-2), we can obtain $\frac{\sigma_N}{\sigma_0}$ of various ξ for different laminate configurations as shown in Column 6 of Tables B-7 to B-9.

B.3 GLASS/EPOXY COMPOSITES (m=.289)

Substituting m=.289 and the test data from Reference 16, as shown in column 4 of Table B-10, into equation (B-1) we obtain \bar{K} as listed in column 5. \bar{K}_Q can be obtained from equation (B-3). By substituting \bar{K}_Q into equation (B-2), we can obtain $\frac{\sigma_N}{\sigma_0}$ for the composite laminate $[0/\pm 45/90]_s$ with both a center crack and a center hole as shown in Column 6 of Tables B-10 and B-11.

Table B-7. Fracture Parameters Of Gr/Ep Laminate $[0/\pm 45]_{2s}$ With Center Crack.

a_0 (mm)	ξ	Y	$\left(\frac{\sigma_N}{\sigma_0}\right)_{\text{Test}}$	R (MPa mm)	$\left(\frac{\sigma_N}{\sigma_0}\right)$	Error %
2.54	.1	1.01	.56	423	.543	-3.0
5.08	.2	1.026	.46	424	.444	-3.4
7.62	.3	1.054	.38	402	.386	1.6
10.16	.4	1.103	.34	409	.34	0
12.7	.5	1.189	.28	386	.296	5.7

$$\bar{K}_Q = \bar{K}_{\text{AVG}} = 408.6 \text{ MPa(mm)}^{.297}$$

$$\sigma_0 = 541 \text{ MPa}$$

NADC-88118-60

Table B-8. Fracture Parameters Of Gr/Ep Laminate [0/±45]_s With Center Crack.

a_0 (mm)	ξ	Y	$\left(\frac{\sigma_N}{\sigma_0}\right)_{\text{Test}}$	\bar{K} (MPa mm)	$\left(\frac{\sigma_N}{\sigma_0}\right)$	Error %
2.54	.1	1.01	.53	397	.526	0.
5.08	.2	1.026	.44	404	.429	-2.5
7.62	.3	1.054	.39	413	.373	-4.5
10.16	.4	1.103	.33	396	.328	-6
12.7	.5	1.89	.26	358	.285	9.7

$$\bar{K}_Q = \bar{K}_{\text{AVG}} = 393.5 \text{ MPa(mm)}^{.297}$$

$$\sigma_0 = 541 \text{ MPa}$$

Table B-9. Fracture Parameters of Gr/Ep Laminate [0/90/±45]_s With Center Crack.

a_0 (mm)	ξ	Y	$\left(\frac{\sigma_N}{\sigma_0}\right)_{\text{Test}}$	\bar{K} (MPa mm) ^{.289}	$\left(\frac{\sigma_N}{\sigma_0}\right)$	Error %
2.54	.1	1.01	.69	464	.662	-4.1
5.08	.2	1.026	.57	454	.552	-3.1
7.62	.3	1.054	.47	424	.484	2.9
10.16	.4	1.103	.416	425	.428	2.8
12.7	.5	1.189	.36	422	.373	3.7

$$\bar{K}_Q = \bar{K}_{\text{AVG}} = 437.7 \text{ MPa(mm)}^{.297}$$

$$\sigma_0 = 454 \text{ MPa}$$

NADC-88118-60

Table B-10. Fracture Parameters of GI/Ep [0/±45/90]_s with a Center Crack.

a_0 (mm)	ξ	Y_c	$\left(\frac{\sigma_N}{\sigma_0}\right)_{\text{Test}}$	\bar{K} (MPa mm) ^{.289}	$\left(\frac{\sigma_N}{\sigma_0}\right)$	Error %
1.45	.11	1.01	.707	283.3	.708	0.
3.86	.30	1.054	.578	305	.530	-8.4
7.37	.29	1.05	.440	268.8	.448	1.0
12.4	.33	1.06	.338	239.4	.382	13.0

$$\bar{K}_Q = \bar{K}_{\text{AVG}} = 274 \text{ MPa(mm)}^{.289}$$

$$\sigma_0 = 320 \text{ MPA}$$

Table B-11. Fracture Strength Prediction of GI/Ep [0/±45/90]_s with a Center Hole.

R_0 (mm)	ξ	Y_H	\bar{K}_Q (MPa mm) ^{.289}	$\left(\frac{\sigma_N}{\sigma_0}\right)_{\text{Test}}$	$\left(\frac{\sigma_N}{\sigma_0}\right)$	Error %
1.27	.1	1.01	274	.696	.709	1.8
3.81	.3	1.054	274	.511	.530	3.6
7.62	.3	1.054	274	.44	.442	.5
12.7	.33	1.06	274	.375	.383	2.0

NADC-88118-60

**APPENDIX C
ANALYTICAL RESULTS OF ANISOTROPIC MODEL**

NADC-88118-60

APPENDIX C. ANALYTICAL RESULTS OF ANISOTROPIC MODEL.

INHERENT FLAW CONCEPT
B/AL ($\pm 45/0_2$)_s EXPONENT = 0.500
UNNOTCHED STRENGTH = 910.5 C₀ = 1.505519

a	$\frac{2a}{w}$	Y	$\left(\frac{\sigma_N}{\sigma_0}\right)^{\text{exp}-1}$	$\left(\frac{\sigma_N}{\sigma_0}\right)$ TEST	$\left(\frac{\sigma_N}{\sigma_0}\right)$ CALC	%ERR
1.25	0.05	1.00579E+00	1.57989E+00	6.19000E-01	7.34908E-01	18.7
2.55	0.05	1.00590E+00	2.54504E+00	5.28000E-01	6.05709E-01	14.7
2.55	0.10	1.01151E+00	2.46633E+00	5.31000E-01	6.02351E-01	13.4
5.10	0.10	1.01151E+00	4.46234E+00	4.23000E-01	4.71975E-01	11.6
7.60	0.30	1.05343E+00	5.91474E+00	3.61000E-01	3.85999E-01	6.9
12.70	0.50	1.18275E+00	1.09092E+01	2.45000E-01	2.75246E-01	12.3
15.25	0.30	1.05379E+00	1.04046E+01	2.81000E-01	2.84453E-01	1.2
25.40	0.50	1.18275E+00	1.66938E+01	2.01000E-01	2.00000E-01	0.5

INHERENT FLAW CONCEPT
B/AL (0/ ± 45)_s EXPONENT = 0.500
UNNOTCHED STRENGTH = 581.4 C₀ = 2.836446

a	$\frac{2a}{w}$	Y	$\left(\frac{\sigma_N}{\sigma_0}\right)^{\text{exp}-1}$	$\left(\frac{\sigma_N}{\sigma_0}\right)$ TEST	$\left(\frac{\sigma_N}{\sigma_0}\right)$ CALC	%ERR
0.65	0.07	1.00787E+00	4.35914E-01	8.28000E-01	8.94933E-01	8.1
1.25	0.05	1.00579E+00	5.60115E-01	7.96000E-01	8.28334E-01	4.1
2.55	0.05	1.00590E+00	1.08791E+00	6.88000E-01	7.21407E-01	4.9
2.55	0.10	1.01151E+00	8.34061E-01	7.30000E-01	7.17407E-01	1.7
5.10	0.10	1.01151E+00	1.54259E+00	6.20000E-01	5.91022E-01	4.7
7.60	0.30	1.05343E+00	3.29595E+00	4.58000E-01	4.94887E-01	8.1
12.70	0.50	1.18275E+00	5.60423E+00	3.29000E-01	3.61259E-01	9.8
15.25	0.30	1.05379E+00	4.27950E+00	4.13000E-01	3.75800E-01	9.0
25.40	0.50	1.18275E+00	8.73365E+00	2.71000E-01	2.67972E-01	1.1

NADC-88118-60

INHERENT FLAW CONCEPT
 B/AL (02/±45)_s EXPONENT = 0.500
 UNNOTCHED STRENGTH = 800.1 C₀ = 1.933202

a	$\frac{2a}{w}$	Y	$\left(\frac{\sigma_N}{\sigma_0}\right)^{\text{exp}-1}$	$\left(\frac{\sigma_N}{\sigma_0}\right)$ TEST	$\left(\frac{\sigma_N}{\sigma_0}\right)$ CALC	%ERR
0.25	0.03	1.00319E+00	2.88986E-01	8.78000E-01	9.38016E-01	6.8
0.65	0.07	1.00787E+00	6.09814E-01	7.82000E-01	8.58330E-01	9.8
1.25	0.05	1.00579E+00	9.01570E-01	7.21000E-01	7.74815E-01	7.5
2.55	0.05	1.00590E+00	1.94803E+00	5.79000E-01	6.52813E-01	12.7
2.55	0.10	1.01151E+00	1.99769E+00	5.71000E-01	6.49194E-01	13.7
5.10	0.10	1.02251E+00	3.53966E+00	4.64000E-01	5.18313E-01	11.7
7.60	0.30	1.05343E+00	4.77558E+00	3.95000E-01	4.27478E-01	8.2
12.70	0.50	1.18275E+00	8.52167E+00	2.74000E-01	3.07310E-01	12.2
15.25	0.30	1.05379E+00	7.76124E+00	3.20600E-01	3.18297E-01	0.7
25.40	0.50	1.18275E+00	1.26673E+01	2.28700E-01	2.24854E-01	1.7

INHERENT FLAW CONCEPT
 B/AL (0)_{6T} EXPONENT = 0.500
 UNNOTCHED STRENGTH = 1672 C₀ = 2.080114

a	$\frac{2a}{w}$	Y	$\left(\frac{\sigma_N}{\sigma_0}\right)^{\text{exp}-1}$	$\left(\frac{\sigma_N}{\sigma_0}\right)$ TEST	$\left(\frac{\sigma_N}{\sigma_0}\right)$ CALC	%ERR
0.25	0.03	1.00319E+00	4.85014E-01	8.18000E-01	9.41832E-01	15.1
0.65	0.07	1.00787E+00	1.10108E+00	6.84500E-01	8.66060E-01	26.5
1.25	0.05	1.00579E+00	1.82059E+00	5.92000E-01	7.85788E-01	32.7
2.55	0.05	1.00590E+00	1.93787E+00	5.80000E-01	6.66334E-01	14.9
2.55	0.10	1.01151E+00	2.17303E+00	5.55000E-01	6.62640E-01	19.4
5.10	0.10	1.01151E+00	3.46239E+00	4.68000E-01	5.32118E-01	13.7
7.60	0.30	1.05343E+00	4.62366E+00	4.00300E-01	4.40046E-01	9.9
12.70	0.50	1.18275E+00	6.44820E+00	3.09800E-01	3.17184E-01	2.4
15.25	0.30	1.05379E+00	8.84757E+00	3.02400E-01	3.28768E-01	8.7
25.40	0.50	1.18275E+00	1.22812E+01	2.32000E-01	2.32617E-01	0.3

DISTRIBUTION LIST

	No. of Copies
Kaman Aerospace..... Attn: Mr. A. Falcone Old Windsor Road Bloomfield, CT 06002	1
NAVAIRDEVCON..... Tom Hess, Code 60C1	1
NAVAIRDEVCON..... Code 6064	3
NAVAIRDEVCON..... Code 8131	2
NAVAIRDEVCON..... Code 6043	25

DISTRIBUTION LIST

No. of Copies

Rockwell International/North American Aircraft Division..... 1
Attn: Mr. W. O'Brien
P.O. Box 92098
Los Angeles, CA 90009

Rockwell International/North American Aircraft Division..... 1
Advanced Technology Program Development
Attn: Dr. Lackman
P.O. Box 92098
Los Angeles, CA 90009

Rockwell International/North American Aircraft Operations..... 1
Attn: Technical Library
P.O. Box 582808
Tulsa, OK 74158

Rockwell International/North American Aircraft Operations..... 1
Attn: Mr. G. Sherrick, Engineering Research and Technology
P.O. Box 582808
Tulsa, OK 74158

Rockwell International/North American Aircraft Operations..... 1
Attn: Mr. M. Whitehead
P.O. Box 582808
Tulsa, OK 74158

Rockwell International/North American Aircraft Operations..... 1
Attn: Mr. F. Kaufman
P.O. Box 582808
Tulsa, OK 74158

Sikorsky Aircraft..... 1
Attn: Technical Library
North Main Street
Stratford, CT 06601-1381

Sikorsky Aircraft..... 1
Attn: Mr. Samuel P. Garbo, MS S314A2
North Main Street
Stratford, CT 06601-1381

Sikorsky Aircraft..... 1
Attn: Mr. T. Cook
North Main Street
Stratford, CT 06601-1381

DISTRIBUTION LIST

	No. of Copies
McDonnell-Douglas Astronautics.....	1
Attn: Mr. C. M. Roe	
5301 Bolsa Avenue	
Huntington Beach, CA 92647	
Northrop Aircraft Corporation.....	1
Attn: Technical Library	
One Northrop Avenue	
Hawthorne, CA 90250	
Northrop Aircraft Corporation.....	1
Attn: Mr. D. Boldi	
One Northrop Avenue	
Hawthorne, CA 90250	
Northrop Aircraft Corporation.....	1
Attn: Dr. M. Ratwani	
One Northrop Avenue	
Hawthorne, CA 90250	
Northrop Aircraft Corporation.....	1
Attn: Mr. B. Butler	
One Northrop Avenue	
Hawthorne, CA 90250	
Northrop Aircraft Corporation.....	1
Attn: Mr. R. Whitehead, Structures Research	
One Northrop Avenue	
Hawthorne, CA 90250	
Rockwell International/North American Aircraft Division.....	1
Attn: Technical Library	
P.O. Box 92098	
Los Angeles, CA 90009	
Rockwell International/North American Aircraft Division.....	1
Attn: Mr. G. Stewart, Advanced Structures Engineering	
P.O. Box 92098	
Los Angeles, CA 90009	
Rockwell International/North American Aircraft Division.....	1
Attn: Mr. A. Sanders	
P.O. Box 92098	
Los Angeles, CA 90009	

DISTRIBUTION LIST

	No. of Copies
McDonnell-Douglas Corporation..... Douglas Aircraft Company Attn: Mr. A. Hawley, Dept. ELH, M/S 212-10 3855 Lakewood Blvd. Long Beach, CA 90846	1
McDonnell-Douglas Corporation..... Douglas Aircraft Company Attn: Mr. R. Petty, Dept. 1L7, M/S 35-98 3855 Lakewood Blvd. Long Beach, CA 90846	1
McDonnell-Douglas Corporation..... Douglas Aircraft Company Attn: Mr. Clifford Y. Kam, Dept. EL8, M/S 212-20 Long Beach, CA 90846	1
McDonnell-Douglas Helicopter Company..... Attn: Technical Library Culver City, CA 90230	1
McDonnell-Douglas Helicopter Company..... Attn: Mr. R. M. Verette Culver City, CA 90230	1
McDonnell-Douglas Helicopter Company..... Attn: Technical Library 5000 E. McDowell Road Mesa, AZ 85205	1
McDonnell-Douglas Helicopter Company..... Attn: Mr. J. K. Sen MS 338, Bldg. 530 5000 E. McDowell Road Mesa, AZ 85205	1
McDonnell-Douglas Helicopter Company..... Attn: Mr. S. Guymon, MS B337 5000 E. McDowell Road Mesa, AZ 85205	1
McDonnell-Douglas Astronautics..... Attn: Technical Library 5301 Bolsa Avenue Huntington Beach, CA 92647	1

DISTRIBUTION LIST

	No. of Copies
LTV Aerospace and Defense Company..... Vought Missiles and Advanced Programs Division Attn: C. Foreman, Engineering Project Manager P.O. Box 655907 Dallas, TX 75265-5907	1
LTV Aerospace and Defense Company..... Vought Missiles and Advanced Programs Division Attn: Mr. R. Knight, MS-TH-83 P.O. Box 650003 Dallas, TX 75265-0003	1
LTV Aircraft Product Group..... Structures Research and Development Attn: Mr. R. Ely, Technical Project Manager P.O. Box 655907 Dallas, TX 75265-5907	1
McDonnell-Douglas Corporation..... Attn: Technical Library P.O. Box 516 St. Louis, MO 63166	1
McDonnell-Douglas Corporation..... Attn: Mr. C. Pingle, Dept. 337, M/S 0644324 P.O. Box 516 St. Louis, MO 63166	1
McDonnell-Douglas Corporation..... Attn: Mr. D. J. Dorr, Dept. 390, M/S 1021310 P.O. Box 516 St. Louis, MO 63166	1
McDonnell-Douglas Corporation..... Attn: Mr. C. Saff, Dept. 337, M/S 0341160 P.O. Box 516 St. Louis, MO 63166	1
McDonnell-Douglas Corporation..... Attn: Mr. T. Hinkel, Dept. 334, M/S 0643063 P.O. Box 516 St. Louis, MO 63166	1
McDonnell-Douglas Corporation..... Douglas Aircraft Company Attn: Technical Library Mail Code 212-10 Long Beach, CA 90846	1

DISTRIBUTION LIST

	No. of Copies
Lockheed Aeronautic Systems Company.....	1
Attn: Mr. E. K. Walker	
P.O. Box 551 - Dept. 76-02, B63, Plt. A1	
Burbank, CA 91520	
Lockheed Aeronautic Systems Company.....	1
Attn: C. F. Griffin, Dept. 76-24	
Advanced Structures Technology Dept.	
Burbank, CA 91520	
Lockheed-Georgia Company.....	1
Attn: Technical Library	
86 South Cobb Drive	
Marietta, GA 30063	
Lockheed-Georgia Company.....	1
Attn: Mr. L. R. Meade, MS 399	
86 South Cobb Drive	
Marietta, GA 30063	
Lockheed-Georgia Company.....	1
Attn: Technical Information	
Dept. 72-34, Zone 26	
Marietta, GA 30063	
Lockheed-Missile and Space Company.....	1
Attn: Technical Library	
1111 Lockheed Way	
Sunnyvale, CA 94088	
Lockheed-Missile and Space Company.....	1
Attn: Mr. J. A. Bailie	
P.O. Box 504, Dept. 81-12, B154	
1111 Lockheed Way	
Sunnyvale, CA 94088	
LIV Aerospace and Defense Company.....	1
Vought AeroProducts Division	
Attn: Technical Library	
P.O. Box 655907	
Dallas, TX 75265-5907	
LIV Aerospace and Defense Company.....	1
Vought AeroProducts Division	
Attn: Mr. J. Pimm, MS 194-51	
P.O. Box 655907	
Dallas, TX 75265-5907	

DISTRIBUTION LIST

	No. of Copies
General Electric Company..... 1 Attn: Dr. B. Rodini P.O. Box 8555-M4018 Philadelphia, PA 19101	1
Grumman Aerospace Corporation..... 1 Attn: Technical Library South Oyster Bay Road Bethpage, Long Island, NY 11714	1
Grumman Aerospace Corporation..... 1 Attn: Mr. R. Hadcock, Advanced Materials South Oyster Bay Road Bethpage, Long Island, NY 11714	1
Grumman Aerospace Corporation..... 1 Attn: Mr. J. Bruno, B44-35 South Oyster Bay Road Bethpage, Long Island, NY 11714	1
Grumman Aerospace Corporation..... 1 Attn: Mr. S. Dastin South Oyster Bay Road Bethpage, Long Island, NY 11714	1
Lockheed Aeronautical Systems Company..... 1 Attn: Technical Library P.O. Box 551 Burbank, CA 91520	1
Lockheed Aeronautical Systems Company..... 1 Attn: C. W. Schneider D/70-03, B-369, P/B-6 P.O. Box 551 Burbank, CA 91520	1
Lockheed Aeronautic Systems Company..... 1 Attn: Mr. D. E. Pettit Rye Canyon Research Lab Burbank, CA 91520	1
Lockheed Aeronautic Systems Company..... 1 Attn: Mr. R. C. Young Rye Canyon Research Lab Burbank, CA 91520	1

DISTRIBUTION LIST

	No. of Copies
General Dynamics/Fort Worth Division.....	1
Attn: Mr. T. Kearns, MS 6217	
P.O. Box 748	
Fort Worth, TX 76101	
General Dynamics/Fort Worth Division.....	1
Attn: Mr. J. A. Fant	
P.O. Box 748 - MZ 2884	
Fort Worth, TX 76101	
General Dynamics/Fort Worth Division.....	1
Attn: Dr. G. Law, Composite Structures Certification	
P.O. Box 748	
Fort Worth, TX 76101	
General Electric Company.....	1
Attn: Technical Library	
1 Neumann Way	
Cincinnati, OH 45215	
General Electric Company.....	1
Attn: Mr. S. Johnson	
1 Neumann Way	
Cincinnati, OH 45215	
General Electric Company.....	1
Attn: Mr. A. W. Kim	
1 Neumann Way	
Cincinnati, OH 45215	
General Electric Company.....	1
Attn: Technical Library	
P.O. Box 8555	
Philadelphia, PA 19101	
General Electric Company.....	1
Attn: Mr. A. Garber	
P.O. Box 8555-M4018	
Philadelphia, PA 19101	
General Electric Company.....	1
Attn: Mr. C. Zweben	
P.O. Box 8555-M4018	
Philadelphia, PA 19101	

DISTRIBUTION LIST

No. of Copies

Boeing Military Aircraft Company..... 1
Attn: Mr. J. Avery
P.O. Box 20746
Wichita, KS 67277-7730

Boeing Military Aircraft Company..... 1
Attn: Mr. R. Waner
P.O. Box 20746
Wichita, KS 67277-7730

Boeing Military Airplane Company..... 1
Attn: Mr. J. Luding, MS K3216
P.O. Box 20746
Wichita, KS 67277-7730

Boeing Military Airplane Company..... 1
Attn: Mr. R. M. Mayle, MS K06-72
P.O. Box 20746
Wichita, KS 67277-7730

General Dynamics/Convair Division..... 1
Space Systems Division
Attn: Technical Library
P.O. Box 85990
San Diego, CA 92138

General Dynamics/Convair Division..... 1
Space Systems Division
Attn: Craig Rix, MZ-23-8443
P.O. Box 85990
San Diego, CA 92138

General Dynamics/Convair Division..... 1
Space Systems Division
Attn: Mr. D. R. Dunbar
P.O. Box 85990
San Diego, CA 92138

General Dynamics/Fort Worth Division..... 1
Attn: Technical Library
P.O. Box 748
Fort Worth, TX 76101

General Dynamics/Fort Worth Division..... 1
Attn: Mr. B. Smith
P.O. Box 748
Fort Worth, TX 76101

DISTRIBUTION LIST

	No. of Copies
Boeing Helicopter Company..... Attn: Mr. D. Hart P.O. Box 16858 Philadelphia, PA 19142	1
Boeing Helicopter Company..... Attn: Mr. R. L. Pinckney P.O. Box 16858 Philadelphia, PA 19142	1
Boeing Helicopter Company..... Attn: Mr. C. Albrecht, MS P32-38 P.O. Box 16858 Philadelphia, PA 19142	1
Boeing Helicopter Company..... Attn: Mr. Brian Lake, MS P30-18 P.O. Box 16858 Philadelphia, PA 19142	1
Boeing Company..... Attn: Technical Library P.O. Box 3707 Seattle, WA 98124-2207	1
Boeing Company..... Attn: Mr. R. Horton P.O. Box 3707-MS 3304 Seattle, WA 98124-2207	1
Boeing Company..... Attn: Mr. M. Cohodas P.O. Box 3707, MS 4A-16 Seattle, WA 98124-2207	1
Boeing Company..... Attn: Mr. J. Quinlivan P.O. Box 3707, MS 6N-21 Seattle, WA 98124-2207	1
Boeing Military Aircraft Company..... Attn: Technical Library P.O. Box 20746 Wichita, KS 67277-7730	1

DISTRIBUTION LIST

No. of Copies

AVCO Specialty Materials - Textron..... 1
Attn: Mr. William F. Grant
Specialty Materials Division
2 Industrial Avenue
Lowell, MA 01851

AVCO Specialty Materials - Textron..... 1
Attn: J. Hemshaw
Specialty Materials Division
2 Industrial Avenue
Lowell, MA 01851

Beech Aircraft Corporation..... 1
Attn: Mr. M. B. Goetz
Claypool Bldg., Office 300
4130 Linden Avenue
Dayton, OH 45432

Beech Aircraft Corporation..... 1
Attn: Mr. M. P. Djuric
Kellogg St. and Webb Road
Wichita, KS 67201

Bell Helicopter/Textron Inc..... 1
Attn: Technical Library
P.O. Box 482
Fort Worth, TX 76101

Bell Helicopter/Textron Inc..... 1
Attn: Mr. D. Reisdorfer
P.O. Box 482
Fort Worth, TX 76101

Bell Helicopter/Textron Inc..... 1
Attn: Mr. M. K. Stevenson
P.O. Box 482
Fort Worth, TX 76101

Boeing Helicopter Company..... 1
Boeing Defense and Space Group
Attn: Dr. C. K. Gunther
P.O. Box 16858, MS P30-30
Philadelphia, PA 19142-0858

Boeing Helicopter Company..... 1
Attn: Technical Library
P.O. Box 16858
Philadelphia, PA 19142

DISTRIBUTION LIST

No. of Copies

Commander..... 1
Naval Aviation Depot
Attn: J. Gresham, Code 35210
MCAS, Cherry Point, NC 28533-5030

Commander..... 1
Naval Aviation Depot
Attn: M. Linn, Code 340
NAS, Jacksonville, FL 32212-0016

Commander..... 1
Naval Aviation Depot
Attn: J. Deans, Code 31310, Bldg. V88
NAS, Norfolk, VA 23511-5899

Commander..... 1
Naval Aviation Depot
Attn: H. Jarrett, Code 32220
NAS, Norfolk, VA 23511-5899

Commander..... 1
Naval Aviation Depot
Attn: H. Sommerfleck, Code 36030
NAS, Norfolk, VA 23511-5899

Commanding Officer..... 1
Naval Aviation Depot
Attn: D. Perl, Code 343
NAS, North Island, San Diego, CA 92135-5112

Commanding Officer..... 1
Naval Aviation Depot
Attn: M. Williams, Code 31327
NAS, North Island, San Diego, CA 92135-5112

Commanding Officer..... 1
Naval Aviation Depot
Attn: D. Knapp, Code 342
NAS, Pensacola, FL 32508-5300

Commander..... 1
United States Naval Academy
Attn: Mechanical Engineering Dept.
Annapolis, MD 21402

DISTRIBUTION LIST

	No. of Copies
Commanding Officer.....	1
U.S. Army R&T Laboratory (ARRADCOM)	
Attn: K. Abelson	
Building 182	
Dover, NJ 07801	
Commanding Officer.....	1
U.S. Army R&T Laboratory (ARRADCOM)	
Attn: R. Bonk	
Building 182	
Dover, NJ 07801	
Commanding Officer.....	1
U.S. Army Applied Technology Lab	
Attn: G. McAllister	
USARTL, (AVRADCOM)	
Fort Eustis, VA 23604-5418	
Commanding Officer.....	1
U.S. Army Applied Technology Lab	
Attn: J. Waller	
USARTL, (AVRADCOM)	
Fort Eustis, VA 23604-5418	
NASA Headquarters.....	1
Attn: G. Seidel	
OAST-Code RM	
Washington, D.C. 20546	
Administrator.....	1
National Aeronautics and Space Administration	
Attn: Airframes Branch, FS 120	
Washington, D.C. 20546	
Administrator.....	1
National Aeronautics and Space Administration	
Langley Research Center	
Attn: Dr. C. P. Blankenship, M/S-188M	
Hampton, VA 23365-5225	
Administrator.....	1
National Aeronautics and Space Administration	
Langley Research Center	
Attn: Mr. C. E. Harris, MS 188E	
Hampton, VA 23365-5225	

DISTRIBUTION LIST

	No. of Copies
Commander.....	1
David Taylor Research Center	
Attn: A. Macander, Code 1720	
Bethesda, MD 20084	
Commander.....	1
David Taylor Research Center	
Attn: E. T. Camponeschi, Code 2844	
Annapolis, MD 21402	
Commander.....	1
David Taylor Research Center	
Attn: R. Crane, Code 2844	
Annapolis, MD 21402	
Commander.....	1
David Taylor Research Center	
Attn: H. Edelstein, Code 2870	
Annapolis, MD 21401	
Commander.....	1
Naval Surface Weapons Center	
Attn: Dr. J. M. Augl	
10901 New Hampshire Avenue	
Silver Spring, MD 20903-5000	
Commander.....	1
Naval Surface Weapons Center	
Attn: Dr. J. Goff, R34	
White Oak Laboratory	
Silver Spring, MD 20910	
Commander.....	1
Naval Aviation Depot	
Attn: N. Amdur, Code 342/N	
NAS, Alameda, CA 94501	
Commander.....	1
Naval Aviation Depot	
Attn: J. Meyers, Code 35110	
MCAS, Cherry Point, NC 28533-5030	
Commander.....	1
Naval Aviation Depot	
Attn: J. Fuss, Code 35430	
MCAS, Cherry Point, NC 28533-5030	

DISTRIBUTION LIST

No. of Copies

Commander..... 1
Naval Air Systems Command
Attn: AIR-53022
Washington, D.C. 20361

Commander..... 1
Naval Air Systems Command
Attn: AIR-53023
Washington, D.C. 20361

Commander..... 1
Naval Air Systems Command
Attn: AIR-5304
Washington, D.C. 20361

Commander..... 1
Naval Air Systems Command
Attn: AIR-530T
Washington, D.C. 20361

Commander..... 1
Naval Sea Systems Command
Attn: Sea-05R
Washington, D.C. 20362-5101

Commander..... 1
Naval Weapons Center
Attn: K. Bailey, Code 338
China Lake, CA 93355

Commander..... 1
Naval Weapons Center
Attn: J. E. Diamond, Code 338
China Lake, CA 93355

Commanding Officer..... 1
Naval Ship Engineering Center
Attn: NSEC 6101E
Arlington, VA 20360

Commander..... 1
David Taylor Research Center
Attn: R. Rockwell, Code 1720-6
Bethesda, MD 20084

DISTRIBUTION LIST

	No. of Copies
Office of Naval Technology.....	1
Attn: W. King, ONT-212	
800 N. Quincy Street	
Arlington, VA 22217	
Office of Naval Research.....	1
Attn: A. K. Vasudevan, Code 1216	
800 N. Quincy Street	
Arlington, VA 22217	
Office of Naval Research.....	1
Attn: Y. Rajapakse, Code 1132SM	
800 N. Quincy Street	
Arlington, VA 22217	
Director.....	1
Naval Research Laboratory	
Attn: Dr. R. Badaliance	
4555 Overlook Avenue, S.W.	
Washington, D.C. 20375	
Director.....	1
Naval Research Laboratory	
Attn: Dr. I. Wolock, Code 6383	
4555 Overlook Avenue, S.W.	
Washington, D.C. 20375-5000	
Director.....	1
Naval Research Laboratory	
Attn: C. Poranski, Code 6122	
4555 Overlook Avenue, S.W.	
Washington, D.C. 20375-5000	
Commander.....	1
Naval Air Systems Command	
Attn: AIR-530	
Washington, D.C. 20361	
Commander.....	1
Naval Air Systems Command	
Attn: AIR-5302	
Washington, D.C. 20361	
Commander.....	1
Naval Air Systems Command	
Attn: AIR-53021	
Washington, D.C. 20361	

DISTRIBUTION LIST

No. of Copies

Administrator..... 1
National Aeronautics and Space Administration
George C. Marshall Space Flight Center
Attn: Technical Library
Huntsville, AL 35812

Administrator..... 1
National Aeronautics and Space Administration
Lewis Research Center
Attn: Dr. C. Chamis, MS-49-6
21000 Brookpark Road
Cleveland, OH 44153

Administrator..... 1
National Aeronautics and Space Administration
Lewis Research Center
Attn: M. Hershberg, MS 49-6
21000 Brookpark Road
Cleveland, OH 44153

Administrator..... 1
National Aeronautics and Space Administration
Lewis Research Center
Attn: Technical Library
21000 Brookpark Road
Cleveland, OH 44153

Administrator..... 2
Defense Technical Information Center
Bldg. #5, Cameron Station
Alexandria, VA 22314

Federal Aviation Administration..... 1
Attn: Mr. J. R. Soderquist, AIR-103
800 Independence Avenue, S.W.
Washington, D.C. 20591

Federal Aviation Administration..... 1
Attn: Mr. L. Neri, Code ACD-210
Technical Center
Atlantic City, NJ 08405

Federal Aviation Administration..... 1
Attn: C. Caiafa, Code ACT-330
Technical Center
Atlantic City, NJ 08405

DISTRIBUTION LIST

No. of Copies

Administrator..... 1
National Aeronautics and Space Administration
Langley Research Center
Attn: Dr. J. Starnes, MS 190
Hampton, VA 23365-5225

Administrator..... 1
National Aeronautics and Space Administration
Langley Research Center
Attn: Dr. M. Mikulas, Code MS 190
Hampton, VA 23365-5225

Administrator..... 1
National Aeronautics and Space Administration
Langley Research Center
Attn: Mr. W. T. Freeman, MS 243
Hampton, VA 23365-5225

Administrator..... 1
National Aeronautics and Space Administration
Langley Research Center
Attn: Mr. J. W. Deaton, MS 188A
Hampton, VA 23365-5225

Administrator..... 1
National Aeronautics and Space Administration
Langley Research Center
Attn: Mr. J. Davis, MS 243/STPO
Hampton, VA 23365-5225

Administrator..... 1
National Aeronautics and Space Administration
Langley Research Center
Attn: Dr. R. Price
Hampton, VA 23365-5225

Administrator..... 1
National Aeronautics and Space Administration
Langley Research Center
Attn: Dr. G. L. Roderick
Hampton, VA 23365-5225

Administrator..... 1
National Aeronautics and Space Administration
George C. Marshall Space Flight Center
Attn: R. Schwingamer, S&E-ASTN-M
Huntsville, AL 35812

DISTRIBUTION LIST

	No. of Copies
Commanding Officer.....	1
Warner Robbins Air Logistics Command	
Attn: T. F. Christian, MMSRD	
Robbins Air Force Base, GA 30198	
Commanding Officer.....	1
Warner Robbins Air Logistics Command	
Attn: W. Schweinberg, MMTRC	
Robbins Air Force Base, GA 30198	
Commanding Officer.....	1
Picatinny Arsenal	
PLASTECH	
Attn: Librarian, Code DRDAR-SCM-0, Bldg. 351N	
Dover, NJ 07801	
Commanding Officer.....	1
U.S. Army Air Mobility R&D Lab	
Attn: H. Reddick	
Fort Eustis, VA 23604	
Commanding Officer.....	1
U.S. Army Aviation Applied Technology Directorate	
Attn: T. E. Condon	
SAVRT/TY-ASR	
Fort Eustis, VA 23604-5577	
Commanding Officer.....	1
U.S. Army Aviation Applied Technology Directorate	
Attn: Drew Orfino	
SAVRT/TY-ATS	
Fort Eustis, VA 23604-5577	
Commanding Officer.....	1
U.S. Army Materials and Mechanical Research Center	
Attn: D. Oplinger, SLCMT-MS	
Watertown, MA 02171-0001	
Commanding Officer.....	1
U.S. Army Research Office	
Durham, NC 27701	
Commanding Officer.....	1
U.S. Army R&T Laboratory (AVRADCOM)	
Attn: F. Immen, Code DAVDL-AS-MS-207-5	
Ames Research Center	
Moffett Field, CA 94035	

DISTRIBUTION LIST

No. of Copies

Commanding Officer..... 1
Wright Research and Development Center
Attn: FIBC/C. Ramsey
Wright Patterson Air Force Base, OH 45433-6553

Commanding Officer..... 1
Wright Research and Development Center
Attn: FIBEC/Dr. G. Sendeckyj
Wright Patterson Air Force Base, OH 45433-6553

Commanding Officer..... 1
Wright Research and Development Center
Attn: FIBR/H. F. Wolfe
Wright Patterson Air Force Base, OH 45433-6553

Commanding Officer..... 1
Wright Research and Development Center
Attn: FIBA/L. Kelly
Wright Patterson Air Force Base, OH 45433-6553

Commanding Officer..... 1
Wright Research and Development Center
Attn: MLBM/Dr. J. Whitney
Wright Patterson Air Force Base, OH 45433-6553

Commanding Officer..... 1
Wright Research and Development Center
Attn: MLSE/S. Fecheck
Wright Patterson Air Force Base, OH 45433-6553

Commanding Officer..... 1
Wright Research and Development Center
Attn: MLBM/Dr. M. Knight
Wright Patterson Air Force Base, OH 45433-6553

Commanding Officer..... 1
Wright Research and Development Center
Attn: MLB/F. Cherry
Wright Patterson Air Force Base, OH 45433-6553

Commanding Officer..... 1
Wright Research and Development Center
Attn: MLSE/T. Reinhart
Wright Patterson Air Force Base, OH 45433-6553

Commanding Officer..... 1
Wright Research and Development Center
Attn: MLIN/R. C. Tomashot
Wright Patterson Air Force Base, OH 45433-6553

DISTRIBUTION LIST

No. of Copies

Commander..... 1
U.S. Naval Postgraduate School
Attn: Professor R. Ball
Monterey, CA 93943

Commander..... 1
U.S. Naval Postgraduate School
Attn: Professor M. H. Bank, Code 67BP
Monterey, CA 93943

Commander..... 1
U.S. Naval Postgraduate School
Attn: Professor K. Challenger
Monterey, CA 93943

Commander..... 1
U.S. Naval Postgraduate School
Attn: Technical Library
Monterey, CA 93943

Commander..... 1
U.S. Naval Postgraduate School
Attn: Dr. E. Robert Wood, Code 67
Monterey, CA 93943

Department of the Air Force..... 1
Attn: Dr. M. Salkind
Building 410
Boiling Air Force Base
Washington, D.C. 20331

Department of the Air Force..... 1
Attn: Dr. J. Amos
Building 410
Boiling Air Force Base
Washington, D.C. 20331

Commanding Officer..... 1
Wright Research and Development Center
Attn: FIBA/W. Goesch
Wright Patterson Air Force Base, OH 45433-6553

Commanding Officer..... 1
Wright Research and Development Center
Attn: FIB/R. Bader
Wright Patterson Air Force Base, OH 45433-6553